ELECTRICAL RESISTIVITY SURVEYS OF APPLIED HOG MANURE SITES, MOUNT JUDEA, AR

Final Report
Jon Fields and Todd Halihan

OKLAHOMA STATE UNIVERSITY
Boone Pickens School of Geology
105 Noble Research Center Stillwater, OK 74078-3031
405.744.6358, FAX 405.744.7841

Table of Contents

List of Figures

List of Tables

1.0 Executive Summary

Electrical Resistivity Imaging (ERI) surveys were conducted in December 2014 and March 2015 to evaluate the application of hog manure in riparian and adjacent areas in the Mount Judea, Arkansas area by defining potential groundwater flowpaths, soil structure, epikarst characteristics, and bedrock properties. ERI surveys generate a two dimensional cross section of geology based on the electrical properties of the subsurface. These properties are controlled by the type of soil or rock at a location and the electrical conductivity of the fluids in the soil. Rock with a low porosity and is competent, will be more resistive than fractured or weathered rock. Soil composed of fine grained material, like clay, is more electrically conductive than sandy soils. Features with more water content or higher salinity are more electrically conductive, while those with less water or salinity are more resistive.

The Phase I survey conducted a preliminary evaluation of applied hog manure in this setting to determine if electrical signatures were generated and could be investigated further. The application of hog manure has the possibility of providing a more electrically conductive signature in soil, which will appear in ERI surveys. These are not distinctly different from other electrically conductive substances in the subsurface; other analysis and sampling must be done to determine if the electrically conductive features are the signatures of hog manure.

The Phase II survey conducted evaluation of the previous fields and introduced another field with a recent application of hog manure. Three sites were compared: a background site with no applied hog manure (Field 5a), a site with application months before data collection (Field 12), and a site with a recent application only weeks before data collection (Field 1). The comparison determined the potential for electrical signatures to delineate the two application fields from each other, and from the background site. Soil sampling was conducted on all three fields as part of the phase II evaluation. The sampling provided a characterization and monitoring method to evaluate possible electrical signatures of applied hog manure.

Fields 5a and 12 were measured in December 2014 and March 2015; Field 1 was measured in March 2015. Field 5a was the background field with no application, Field 12 had a hog manure application in April 2014 and Field 1 received a hog manure application sometime in January or February 2015. Several datasets were collected and the following observations were made from the ERI data:

- ERI provided delineation of boundaries between soil, epikarst, and competent bedrock.
- The potential for rapid transport pathways in the underlying bedrock as joints or potential karst features were observed as conductive electrical features in a resistive background.
- Soil depth was measured to range from 0.5 to 3.5 meters (1.5 to 11.5 feet). On Fields 5a and 12, the thickness of soil increases moving toward the stream and thins towards higher elevations. This is consistent with the thickening of the alluvium as it is deposited closest to the stream.
- The average epikarst thickness is highly variable, ranging from 2.0 to 23.0 meters thick (6.0 to 75.0 feet).

- Soils of the background site (Field 5a) were lower in Zn in the soil solids, and lower in Mg and electrical conductivity in the soil fluids when compared to the results of the applied sites (Fields 12 and 1).
- Soils of the recently applied site (Field 1) were higher in K, Mn, and pH in the soil solids, and higher in K and pH in the soil fluids when compared to the results of the other two sites (Fields 5a and 12).
- There is a correlation between the spatial application of hog manure and increased electrical conductivity in the ERI and soil sampling results.
- There is an inverse relationship between the 0.5-meter resolution ERI bulk resistivity and soil fluid electrical conductivity at the background site. The applied sites have a direct relationship.

2.0 Glossary

This section includes the definitions for heavily used technical terms throughout this report. Accompanying many definitions are abbreviations for the references (WS – Water Science Glossary; GG – Geologic Glossary; UT – Glossary of Hydrological Terms; ES – A Dictionary of Earth Science; CK – A Lexicon of Cave and Karst Terminology; NOAA – National Oceanic and Atmospheric Administration; TH – ERI of the Arbuckle Simpson Aquifer)

Alluvium: deposits of clay, silt, sand, gravel, or other particulate material deposited by a stream or other body of running water in a streambed, on a flood plain, on a delta, or at the base of a mountain. (WS)

Apparent Resistivity: the resistance per length of a surface area, in essence the resistance of a cube to the one-way passage of electricity – this is used in many geophysical and hydrogeological applications. (UT)

Carbonates: frequently used with reference to sedimentary rocks composed of 95% or more of either calcite or dolomite – examples include limestone and dolomite. (ES)

Conductive Fluid: fluid that readily conducts electricity – the degree to which the fluid is conductive depends on the concentration of dissolved ions within the fluid – examples include sodium and chloride ions from dissolving table salt in water. (TH)

Disconformity: buried erosional surface representing a break in the geologic record of significant time but one which the beds above and below the surface are parallel; some disconformity surfaces are highly irregular, whereas others have no obvious relief. (ES)

Dissolution Feature: dissolution is the process in which a solid becomes dissolved in (ground) water– dissolution features include caves, sinkholes, enlarged fractures, and doline features. (UT)

Doline Feature: a closed topographic depression caused by dissolution or collapse of underlying rock or soil; synonymous with sinkhole. (UT)

Epikarst: a relatively thick portion of bedrock extending from the base of the soil zone and is characterized by extreme weathering and enhanced solution. Thickness may vary considerably; may be up to 30 meters thick. Significant water storage and transport are known to occur in this zone. (CK)

ERI: Electrical Resistivity Imaging – a geophysical method where an electrical current is injected into the ground through two electrodes; the resulting electrical potential is measured between two separate electrodes and the apparent resistivity is calculated. Thousands of these measurements allow for imaging of the subsurface. (TH)

Fault: a fracture in the Earth along which one side has moved relative to the other. (GG)

Flowpath: the subsurface course a water molecule or solute would follow in a given ground-water velocity field. (CK)

Fracture: a break or secondary discontinuity in the rock mass, whether or not there has been relative movement across it. Faults, thrusts, and joints are all fractures. Bedding planes are primary features and are not considered fractures. (CK)

GPS: Global Positioning System – a space based satellite navigation system that gives time and location anywhere on the Earth where there is an unobstructed line of sight with four or more satellites.

Groundwater: water that flows or seeps downward and saturates soil or rock, supplying springs and wells. Water stored underground in rock crevices and in the pores of geologic materials that make up the Earth's crust. The upper surface of the saturated zone is called the water table. (WS)

Joint: a break of geological origin in the continuity of a rock body occurring either singly, or more frequently in a set or system. The break is not attended by a visible movement parallel to the surface of the discontinuity. (CK)

Karst: the result of natural processes in and on the Earth's crust caused by dissolution and leaching of limestones, dolomites, gypsum, halite, and other soluble rocks. (CK)

Limestone: a sedimentary rock made mostly of the mineral calcite; it is usually formed from shells of once-living organisms or other organic processes, but may also form by inorganic precipitation. (GG)

OPUS: Online Positioning User Service – a service run by the National Geodetic Survey (NGS) as part of the National Oceanic and Atmospheric Administration (NOAA). The service solves the GPS position of the user by tying the survey-grade data to the National Spatial Reference System (NSRS). (NOAA)

Perched Groundwater: unconfined groundwater separated from an underlying body of groundwater by an unsaturated zone. The perching bed permeability is so low water percolating downward through it is not able to bring water in the underlying unsaturated zone above atmospheric pressure. (CK)

Perched Water Table: the water table for the perched groundwater. The upper surface of the perched groundwater. (CK)

Resistive Feature: fluids and rock bodies that do not readily conduct electricity – the degree to which a feature is resistive depends on porosity, salt content in the fluid, and rock or soil type. (TH)

Root Mean Square Error: is the average of the squares of the "errors", the difference between the estimator and what is estimated.

Sandstone: a clastic sedimentary rock composed of sand sized grains. (GG)

Soil Zone: the zone between the ground surface and the epikarst. Water is able to pass through this zone to reach the water table. (ES)

Quaternary: the most recent Period in the Cenozoic Era and encompasses the time interval of 1.6 million years ago through today. (GG)

Water Table: the upper surface of a zone of saturation except where that surface is formed by a confining unit; where the water pressure in porous medium equals atmospheric pressure. (CK)

3.0 Introduction

The purpose of this report is to document the results of a three-dimensional geophysical site characterization of three fields adjacent to Big Creek, which received hog manure applications or have the potential to receive it. This report defines the subsurface geoelectrical properties of three fields near Mount Judea, Arkansas in December 2014 and March 2015. One field (Field 5a) was selected to measure background data on the soil and subsurface environment, but has not yet received any hog manure. A second site (Field 12) was selected, where hog manure was applied in April 2014. A third site (Field 1) was selected, where hog manure was applied between January and February 2015.

3.1 Electrical Resistivity Imaging

Electrical resistivity imaging (ERI) provided a good method to understand the distribution of fluids and rock properties in the subsurface environment, especially in the presence of fractures (Bolyard, 2007; Gary et al., 2009; Halihan et al., 2009). The method allows an electrical image to be created of the subsurface, which typically provides a meter-scale dataset utilized to evaluate heterogeneity and fluid distribution. Improvements in sensitivity generated by the Halihan/Fenstemaker method (OSU Office of Intellectual Property, 2004), allow greater differentiation of these signatures (Miller et al., 2014). In a field setting, this results in a two-dimensional mapping of subsurface electrical properties in vertical cross sections. Data interpolation was utilized to construct horizon map data at various depths below the surface.

Figure 1 - Electrical resistivity equipment during data collection (12.17.14)

3.2 Soil Sampling

Soil sampling transects in each field provided confirmation data to support the geophysical datasets. Soil sampling has been used to characterize the physical and chemical properties of soils (Anderson, 1960; Schoenau, 2006). The University of Arkansas Soils Testing

and Research Laboratory and Oklahoma State University's (OSU) Soil, Water and Forage Analytical Laboratory were used for testing the soils collected in the field. Samples were analyzed for fluid and solid chemical composition using the 1:1 soil-water extraction method and Mehlich-3 extraction method, respectively, to determine if signatures of applied hog manure were evident in the soil. OSU's School of Geology geochemistry laboratory was utilized for isotope ratio mass spectrometry analysis, to determine if the $\delta^{15}N/^{14}N$ ratios of the samples matched those of hog manure. Soil sampling data were compared against the electrical resistivity data to evaluate how the soil physical and chemical properties affected the geophysical signatures observed for the sites.

3.3 Project Statement

This report documents a geophysical investigation of three sites along Big Creek near Mount Judea, Arkansas using electrical resistivity and soil sampling datasets. It describes the field sites and literature available for methods utilized and properties of applied hog manure. The results of the study will be presented with the geologic and hydrogeologic structure evaluated from the electrical data. The soil data results will be presented and correlations among datasets will be evaluated and discussed. Conclusions about the electrical resistivity and soil sampling datasets will be made at the end of this report.

4.0 Site Description and Selection

The three test sites (Fields 1, 5a, and 12) are given in Figure 2. These three sites were chosen to coincide with additional surface water quality monitoring on these fields by the University of Arkansas Big Creek Research and Extension Team. Access to the sites was granted by the landowners. The positions of the selected sites are representative of fields adjacent to Big Creek which are permitted to receive hog manure. Field 5a (background site) currently receives mineral fertilizers and poultry litter, while Field 12 (application site) received one application of hog manure in late April of 2014, and Field 1 (recent application site) has received two applications of hog manure with the most recent being between January and February of 2015. This section will describe the geologic and hydrologic settings of three test sites.
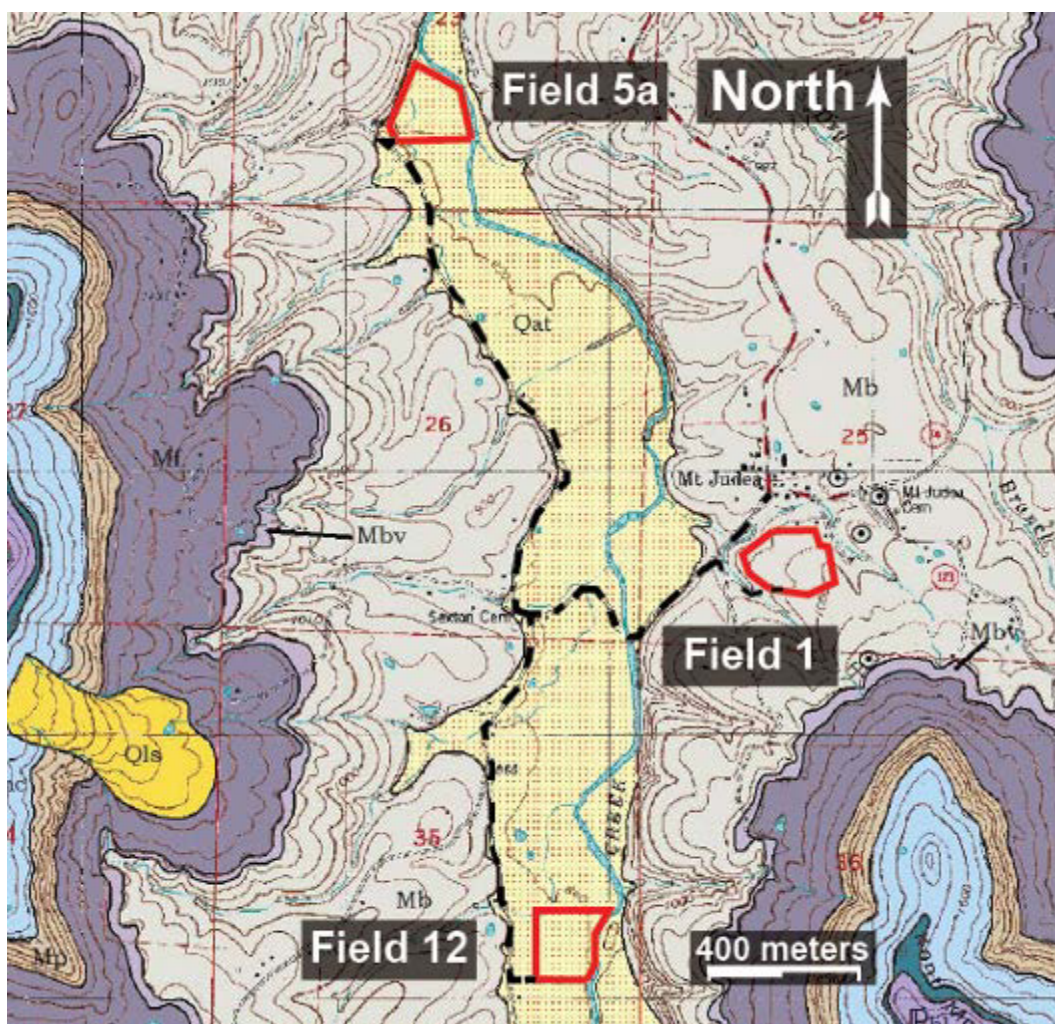
Figure 2 – Site map indicating the three fields (Field 1, 5a, and 12) in red and roads leading to these sites in dashed black lines. The Geologic map of the Mt. Judea Quadrangle, Newton County, Arkansas is from Chandler and Ausbrooks, revised 2015.

4.1 Geologic Setting

The geologic setting for the sites is mantled epikarst (soil over epikarst over competent carbonate bedrock). Fields 5a and 12 sit on Quaternary alluvium deposits, while Field 1 sits on a fine- to coarse-grained fossiliferous limestone with interbedded chert. The Boone Formation is the underlying bedrock for each site. The geologic setting for Fields 1, 5a, and 12 are detailed below.

Fields 5a and 12 (Figures 3 and 4, respectively) share similar geologic settings adjacent to Big Creek (Figure 2). The alluvium at the surface of both sites consists of clay, silt, sand, and gravel deposited by Big Creek. Alluvium can be organic rich and flat lying; good for use as cropland. Underlying the alluvium is an epikarst system and underlying unweathered limestone bedrock (Williams, 2008). Epikarst is a zone extending from the base of the soil zone to the unweathered portion of the limestone bedrock and is characterized by fracturing and weathered bedrock (Klimchouk et. al., 2004). This zone is generally a domain with faster fluid flow and greater water storage than the unweathered bedrock, with distinct saturation at the soil and epikarst boundary and again at the epikarst and karst boundary (Perrin et. at., 2003). General epikarst porosity ranges from 1% (Smart et. al., 1986) to 10% (Williams, 1985) and averages about 10 – 15 meters (33 – 49 feet) in depth (Klimchouk et. al., 2004).

Field 1 (Figure 5) is located on a hillside about 400 m from Big Creek and underlain by the Boone Formation. It is an Early Mississippian Period limestone found in the Ozark regions of Eastern Oklahoma, Southern Missouri, and Northern Arkansas where karst dissolution features including sinkholes, caves, and enlarged fissures are common (Ferguson, 1920). This formation averages 90 – 120 meters (300 – 400 feet) thick (Ferguson, 1920).

The Boone Formation is a gray, fine to coarse-grained fossiliferous limestone with interbedded dark and light chert. The basal unit of the Boone Formation in the area is the St. Joe Limestone (Ferguson, 1920). The St. Joe is a fine-grained, crinoidal limestone containing some smoothly bedded chert and displaying coarse bioclastic texture. The color is generally gray but can be red, pink, purple, brown, or amber. Thin calcareous shales can be found in sequences throughout the St. Joe. The base of the St. Joe contains phosphate nodules within a green shale or conglomerate and is disconformable in most places. At a few locations, basal sandstone is found at the base of the St. Joe Limestone. The basal sandstone is a fine to medium-grained, moderately sorted, sub-rounded to rounded sandstone. It is white to light gray and tan on fresh surfaces, thin to thick bedded, and contains phosphate nodules and white to light gray chert. It is generally up to 3.5 meters (12 feet) thick (Ferguson, 1920). The Boone Formation is the bedrock at all three sites, but Field 1 is missing the alluvium Fields 5a and 12 have above the bedrock.
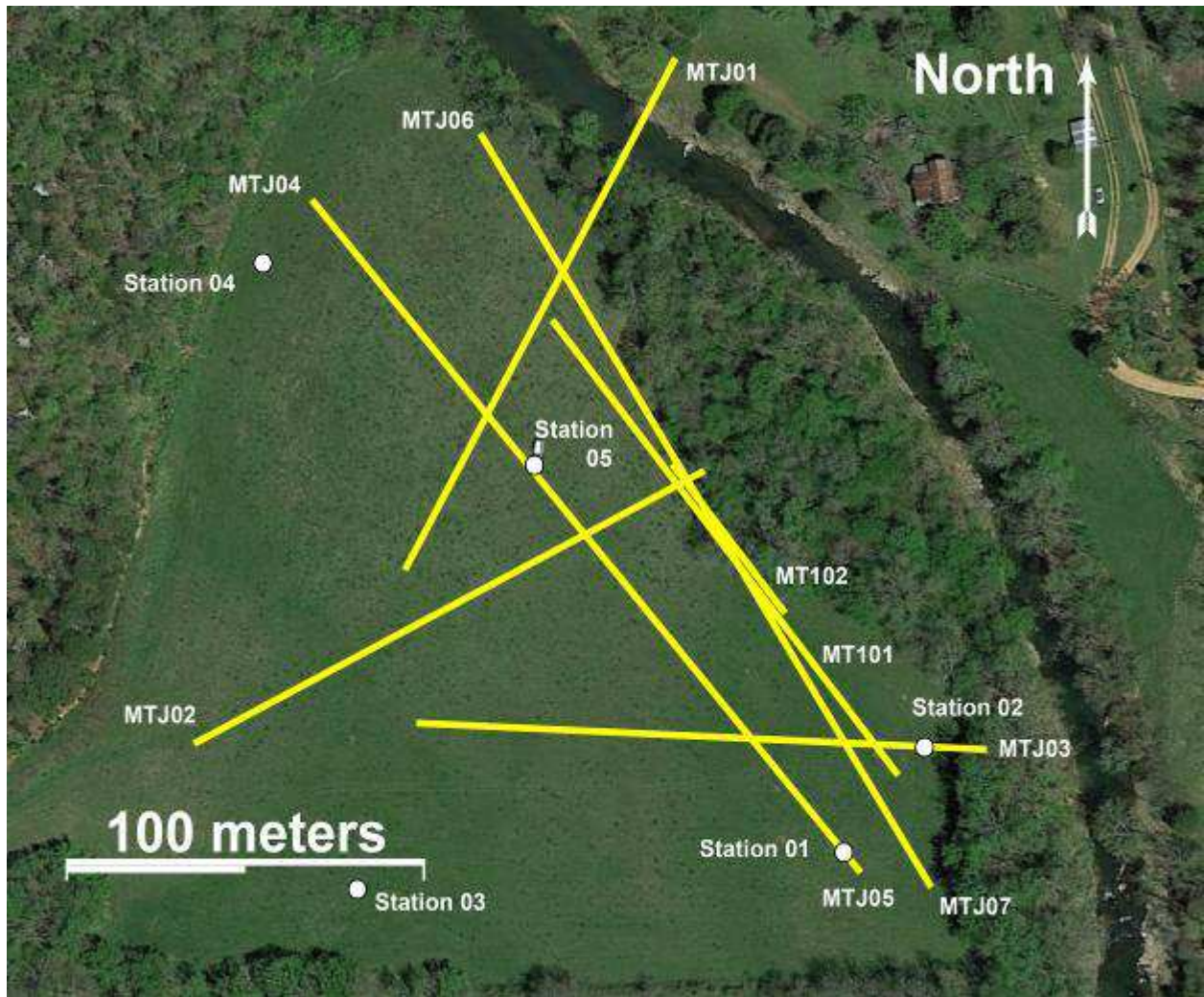
Figure 3 – Field 5a (background site) ERI transects collected during December 2014 and March 2015 are in yellow, shallow well locations (stations) also noted. Aerial photo obtained from Google Earth.
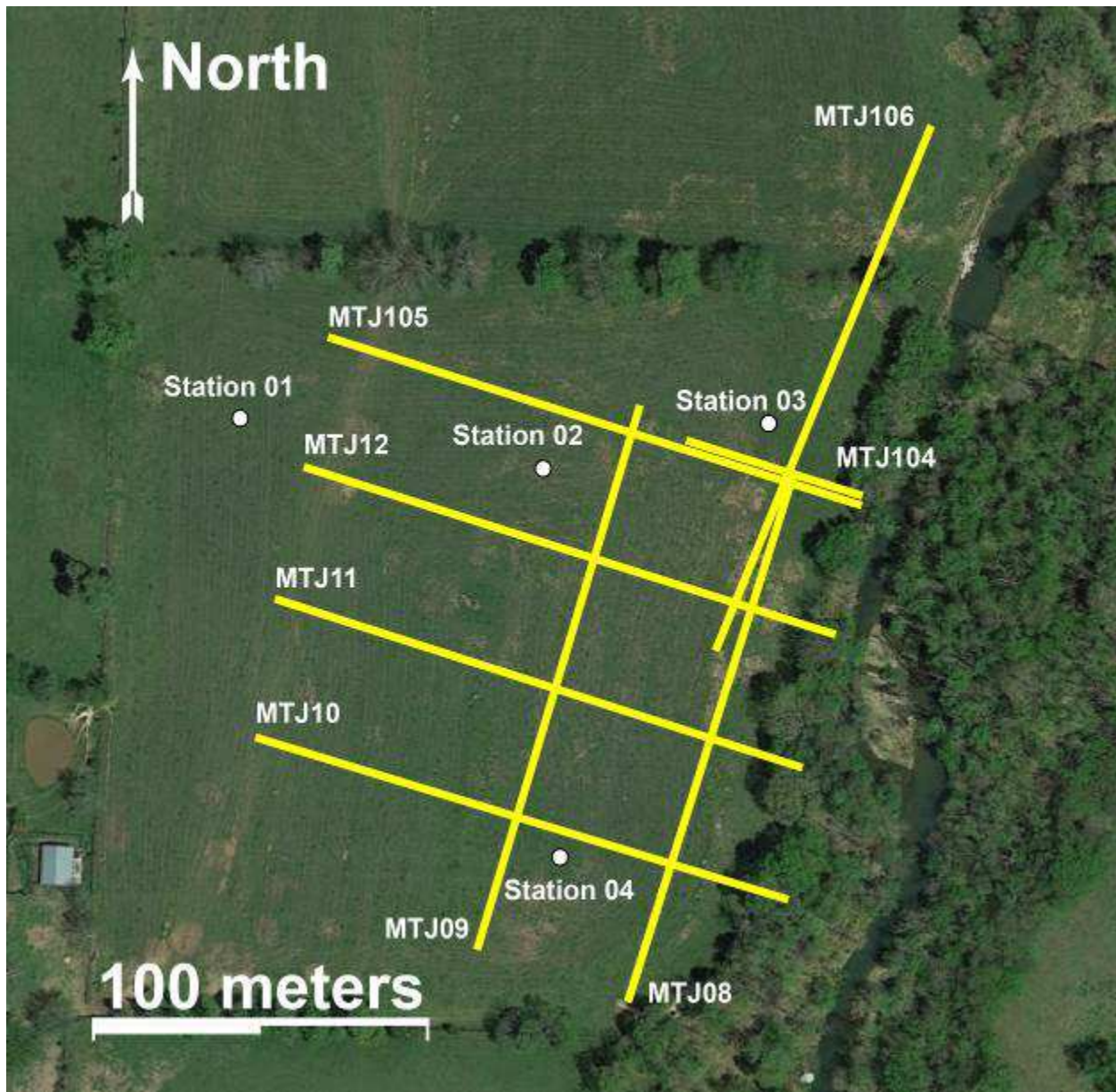
Figure 4 – Field 12 (application site) ERI transects collected during December 2014 and March 2015 are in yellow, shallow well locations (stations) also noted. Aerial photo obtained from Google Earth.
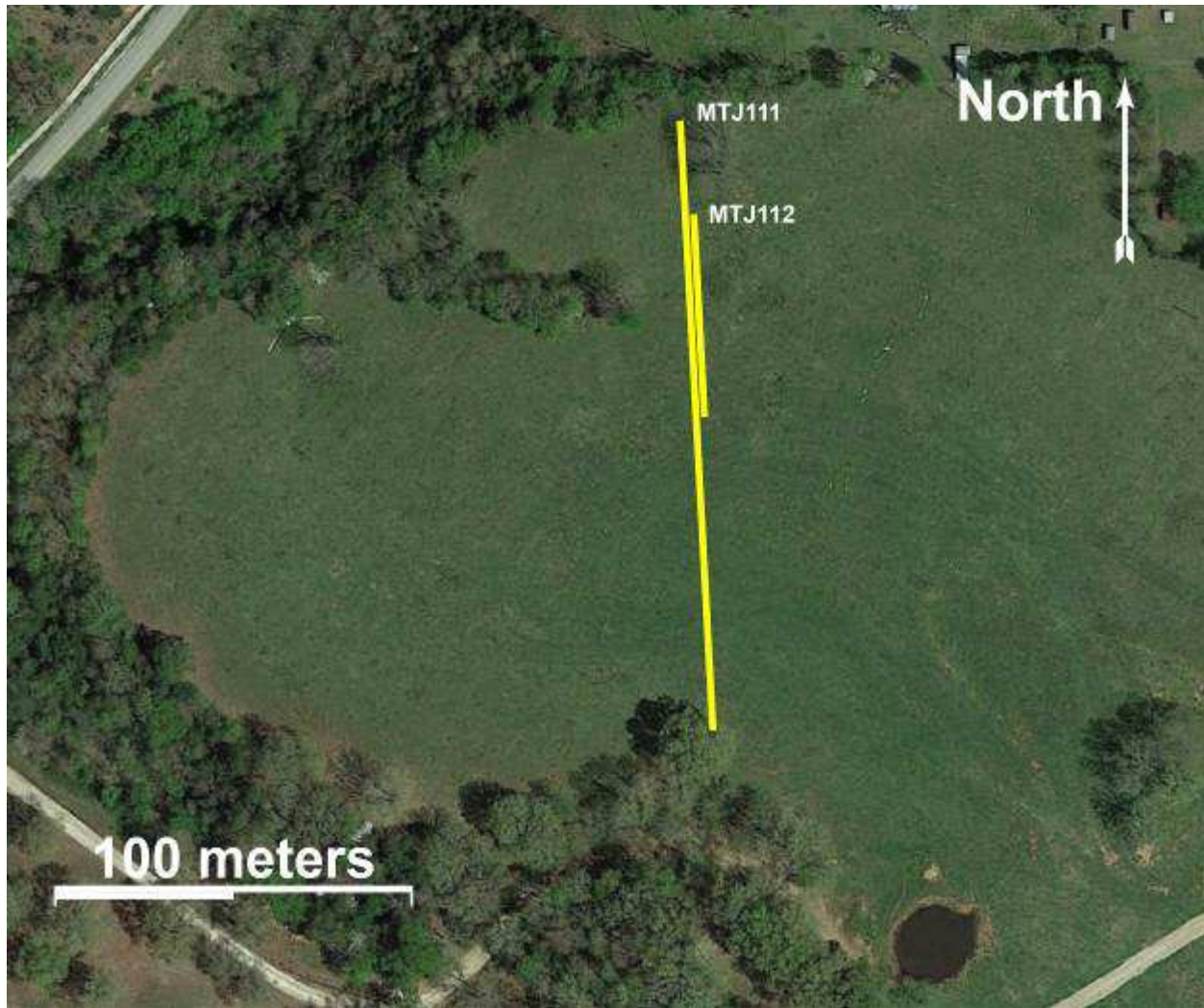
Figure 5 – Field 1 (recent application site) ERI transects collected during March 2015 are in yellow. Aerial photo obtained from Google Earth.

4.2 Hydrologic Setting

The hydrologic setting for the sites is a mantled epikarst (soil over epikarst over competent carbonate bedrock). Precipitation enters the subsurface through the soil zone and enters the epikarst area. Fluids move through the epikarst area and enter the unweathered competent bedrock through fractures and other openings. Understanding the storage and transmission properties of these three zones is essential to understanding the migration of nutrients from applied hog manure in the area. This section will discuss the hydrologic settings of the soil zone, epikarst zone, bedrock, the local water table and the application of hog manure at the time of data collection.

The soil zones in an alluvial setting are often reworked stream deposits that have been mobilized several times since they were originally deposited. They are often highly variable in grain size and organic content. Silt-sized grains in Fields 5a and 12 should result in the ability of the soil to hold fluids for some period of time. The soil zones in an epikarst environment are thin and often contain rock within the zone near the surface. The soil zone consistency is sporadic as

the hydrological processes erode areas at differing rates. The soil and epikarst interface in Field 1 is shallower than Fields 5a and 12, resulting in the potential for less soil filtering that the other sites prior to fluids entering into the epikarst zone.

In geologic settings like northern Arkansas, the epikarst zone is a significant source of water storage and transmission and many springs have been tapped to support local communities (Galloway, 2004). These types of groundwater systems can include perched water tables, which exist above regional water tables. These are called perched because they are places where low permeability soil or bedrock layers hold water above an unsaturated zone and often produce springs on the side of a bluff or sometimes in an open field if the relief is high enough to expose this feature. The boundary of the soil zone with the epikarst zone is visible in some locations in the fields used for this study. Perched features are not apparent at either site. This zone is expected to have wide variability in flow rates and a high amount of storage (Williams, 2008). There can be slow seepage through weathered pores and pieces of less weathered bedrock, to relatively rapid flow through fractures and karst features. The electrical features measured at these sites generally indicate high porosity zones and the extent of weathering in these locations (Williams, 2008; Halihan et al, 2009).

Flow through the bedrock will depend on the location of fractures or karst features. Flowpaths will most commonly be electrically conductive relative to the unweathered bedrock beneath the water table. In settings with little dissolution and strong faulting or fracturing, the flowpaths will appear as linear features in ERI datasets (Halihan et al, 2009), but in the event of karst features, they can appear wider (Bolyard, 2007; Gary et al., 2009). Fractures or karst flowpaths present in the bedrock can be localized or but often follow larger regional trends.

The regional water table was not evaluated for this report but at the two sites on the alluvium, the local water table was shallow during the investigation. For Field 5a, the depth to the local water table was approximately 1.5 meters (5 feet) below the land surface. For Field 12, the local water table was approximately 2 meters (6.5 feet) below the surface. The local water table was not detected in Field 1. Precipitation previous to and during the investigation resulted in both sites having moist to saturated soil conditions. The site soil of Field 1 was saturated.

Farm manure application records show that slurry was applied to Fields 12 and 1 but not 5a. Field 12 received one application in April 2014 of 48,000 gallons (182 meters^3) spread over 9.9 acres (40,064 meters^2) for an application flux of 0.18 inches (0.5 centimeters) of applied manure. This application was eleven months prior to sampling for both ERI and soil composition. Field 1 received four applications of applied manure. Total application was 82,000 gallons (310 meters^3) over an average of 6.9 acres (27,923 meters^2), which provides a total flux of 0.44 inches (1.1 centimeters) prior to sampling. The latest application before ERI and soil sampling was in January or February 2015 when 21,000 gallons (79 meters^3) were applied to 7.3 acres (29,542 meters^2) resulting in an event flux of 0.11 inches (0.3 centimeters) approximately a month prior to sampling. The applied material was electrically conductive fluid with reported conductivities ranging from 8,410 to 12,890 micromhos/cm.

5.0 Methods

As part of this assessment, Oklahoma State University (OSU) designed and conducted ERI experiments to integrate the ERI data with site data and soil data to provide an understanding of the subsurface distribution of flowpaths on Fields 5a, 12, and 1. Field methods included ERI surveys, topographic site surveying using differential GPS (global positioning system) techniques, and soil sampling along ERI surveys. The experimental design was based on observing changes between applied and unapplied fields to determine if changes correlated to changes in electrical properties. The sampling was not intended to test or evaluate if levels of measured constituents were at levels above or below any recommended concentrations as other studies concerned with that issue were sampling these same sites.

5.1 General Field and Laboratory Methods

The general methods used to collect the ERI, GPS, and soil sampling data are given below followed by site-specific descriptions of the methods used.

5.1.1 ERI Data

ERI data collection requires special instruments and transect planning. The ERI data collection instrumentation used was an Advanced Geosciences, Inc. (AGI) SuperSting R8/IP resistivity instrument. The instrument is a multi-channel earth resistivity meter with memory storage. The multi-channel design allows for measuring times to be decreased. The project design for Phase I from OSU was to use 56 electrodes at 3-meter spacing (9.8 feet). This spacing allowed for detailed data collection at 1.5-meter (4.9 feet) resolution for a lateral distance of 165-meters (541 feet) and a depth of investigation of 33 meters (108 feet) for each image. The design for Phase II was to use 56 electrodes at both 3-meter spacing (9.8 feet) and 1-meter spacing (3.3 feet). This spacing allowed for the same 1.5-meter resolution data along three lines as in Phase I, but also allowed for data collection at 0.5-meter (1.6 feet) resolution for the lateral distance of 55 meters (180 feet) and a depth of investigation of 11 meters (36 feet) for three separate lines. The spacing is dependent upon balancing the depth of investigation with how much resolution is needed.

Each ERI line was placed using field measuring tapes to 165 meters (541 feet) or 55 meters (180 feet). For each line, 56 stainless steel stakes were inserted into the soil approximately 1-foot deep oriented in a straight line. The resistivity cable was laid out and each electrode on the cable was connected to each stake. The cables were connected to the instrumentation once the line was laid out. A generator and an AGI 12-volt power supply were used to power the instrument. Electrical testing was ready to begin after transects were set up.

Tests were run on the instrument and cable to ensure each electrode was properly connected to each stake and the instrument was running properly. Contact resistance tests were conducted to ensure the circuits were complete. Electrodes with contact resistance greater than 2,000 ohms fail the test and those stakes were either pushed deeper in the soil to help create a better contact with the soil, or an electrically conductive fluid like salt water was poured around the stake to improve contact between the stake and underlying soil. Lower contact resistance indicates better contact with subsurface material, increasing signal strength and improving better data quality and accuracy. With the high soil moisture at the site during the surveys, no extra

fluids were required to obtain good electrode contact. ERI data collection could begin after tests are concluded.

The collected data were evaluated for data quality prior to departing the field. In the laboratory, field electrical data were paired with topographic data and processes to determine 2D resistivity surveys beneath the electrode lines. Data from individual depth horizons were extracted from individual datasets and interpolated to generate depth slices of the site data to provide map views of the site electrical structure. Both 2D vertical and horizontal data were visualized using RockWorks software.

5.1.2 Site Topographic Surveying

Topographic surveys were required for generating the two-dimensional cross-sections produced from the ERI data as well as created a site topographic map. The GPS used for site surveying was a Topcon Positioning Systems, Inc. HyperLite GNSS Base and Rover with Bluetooth connected handheld unit. Personal GPS units come to within approximately 3 meters (10 feet) of a person's true location, but this commercial grade instrument provides locations to within approximately a centimeter (1/2 inch) of its true location. This instrument was set up by positioning a base receiver and utilizing a second mobile receiver to obtain data. Tree cover can be problematic for the Rover to obtain satellite data. At times, points cannot be collected because the Rover was under too much tree canopy. This was the case on both sites near the stream (i.e., Big Creek) and along the site boundaries if tree canopy was dense. The majority of the data were collected in open field conditions, allowing good coverage of the ERI locations.

5.1.3 Soil Sampling

Soil sampling was conducted using a field kit, a list of criteria to be met, and evenly proportioned among the three sites. The soil sampling equipment used was an AMS Basic Soil Sampling Kit which included of a 3 ¼" hand auger tool. The samples were collected to a depth of 0.1 meters (4 inches). Samples were placed in zip-lock bags and stored in a cooler until analysis. The locations for sampling were based on a few criteria: samples were collected at 0.25 meters (9.8 inches) away from an ERI electrode to improve the fit between both the soil sampling and modeled ERI sets of bulk resistivity data. The remaining criteria were chosen on a field-by-field basis. Field 5a consisted of 10 samples correlating to distances along transect MTJ101 (Figure 6) and an attempt to sample across a known soil contact. Field 12 consisted of 11 samples, three of which are in the unapplied area of the field, correlating to distances along transect MTJ105 (Figure 7). Field 1 consisted of 10 samples, one of which is in the unapplied area of the field, that correlate to distances along transect MTJ111 (Figure 8). After collection, the soil samples were submitted for analysis.

Soil samples were analyzed for the chemistry of the soil solids and grain size of the samples by the University of Arkansas Soil Testing and Research Laboratory using the Mehlich-3 extraction method and sieve analysis (Mehlich, 1984). The Mehlich-3 extraction method provided results for the following constituents for the soil solids: pH, phosphorous (P), potassium (K), calcium (Ca), magnesium (Mg), sodium (Na), sulfate (SO_4), iron (Fe), manganese (Mn), copper (Cu), zinc (Zn), and boron (B).

Soil samples were analyzed for soil fluid chemistry by Oklahoma State University's Soil, Water and Forage Analytical Laboratory using a 1:1 soil-water extraction method as part of a soil salinity management test (Klute, 1986; U.S. Salinity Laboratory Staff, 1954). The 1:1 soil-water extraction method provided the following constituents for the soil fluids: pH, potassium

(K), calcium (Ca), sodium (Na), magnesium (Mg), electrical conductivity (EC), total soluble salts (TSS), potassium adsorption ratio (PAR), sodium adsorption ratio (SAR), exchangeable potassium percent (EPP), and exchangeable sodium percent (ESP).

The OSU School of Geology conducted isotopic ratio mass spectrometry (IRMS) analysis for nitrogen isotope ratios of the soil samples. The IRMS analysis provided isotopic composition of the soil which was cross-referenced with that of known isotopic values for hog manure. Samples were placed into tin capsules, weighed, and formed into spheres before being combusted by an Elemental Analyzer (EA). The EA converted the samples to N_2 gas and passed them through the IRMS where the ion ratios were measured. Reference samples, blank tins, and doubles of each sample were run to ensure accuracy of the machine. The resulting data then underwent correction procedures using values of the reference samples (De Groot, 2004).

5.2 Site Methods

These were the field methods applied at each site utilized in the study. Three sites are described for both ERI and soil data collection.

5.2.1 Field 5a

In December 2014, seven ERI transects (MTJ01 - MTJ07) were collected at Field 5a (Figure 3). Three transects ran approximately east-west, while the other four transects ran approximately north-south. Transects were 165 meters long and with 3-meter spacing to share a similar depth of investigation. Transect MTJ01 was the sole transect to cross Big Creek (Figure 14). Transects MTJ02 and MTJ03 were oriented at an angle to MTJ01 but both shared the east-west trend. MTJ04 and MTJ05 were two of the four that ran north-south and were paired to create a longer total transect. These transects ran roughly parallel to the stream and the fence line, and crossed the three east-west trending transects. MTJ06 and MTJ07 were very similar to MTJ04 and MTJ05. They also ran parallel to the stream and fence line, and crossed the three east-west trending transects, but the pair of transects sat approximately 75 meters to the east of MTJ04 and MTJ05. Together, these datasets allowed coverage of Field 5a to evaluate the geologic context of the area.

In March 2015, two ERI transects (MTJ101 & MTJ102) were collected at Field 5a (Figure 3). The two transects were in the same orientation as some surveys in from December, approximately north-south and parallel to the stream. The transects were collinear, sharing similar stake locations and both sat atop the MTJ106 and MTJ107 transects which were run during December at this site. MTJ101 was 165 meters long with 3-meter spacing to share the same depth of investigation as the previous surveys taken on Field 5a. MTJ102 was 55 meters long with 1-meter spacing for a higher resolution of the same area as MTJ101. Soil sample locations for the background site (Field 5a) were chosen based on the Phase I ERI results of MTJ106/MTJ107.

The Phase I data indicated a possible change in soil characteristics from a thin and rocky soil in the northern part of the field to a thicker soil in the southern part of the field. When conducting the statistical analysis on the data, this change in soil characteristics was used to separate the data into two groups. The sample locations for this site were selected in order to capture the possible soil profile change. The samples correlate to distances along MTJ101 (Figure 6). The separation of the soil samples into the thin, rocky northern half and the thicker southern half was split in the middle at the 82.5-meter mark. Five samples fall in the northern half (0 – 82.5 m) and five samples fall in the southern half (82.5 – 165 m).

Figure 6 – Black dots represent soil sample locations along transect MTJ101 (blue line) in Field 5a (background site). Yellow lines represent other ERI lines collected at site.

5.2.2 Field 12

In December 2014, five ERI transects were collected from Field 12 (MTJ08-MTJ12) (Figure 4). Three of transects ran approximately east-west, while the other two transects ran north-south. Transects were 165 meters long with 3-meter spacing to share a similar depth of investigation. Transects MTJ08 and MTJ09 ran parallel to each other and nearly parallel to Big Creek, covering almost the entire length of the field. Transects MTJ10, MTJ11, and MTJ12 ran perpendicular to MTJ08 and MTJ09. All three were parallel to each other and the fence line. These three ran north-south and were separated from each other by approximately 40 meters. This set of transects covered a sufficient area of the field to evaluate the geologic objectives and covered the boundary between the unapplied edge of the field and application zone in the center of the field.

In March 2015, three ERI transects (MTJ104 - MTJ106) were collected at Field 12 (Figure 4). Two transects were in the same orientation as the surveys in December, approximately east-west and perpendicular to the stream. The transects were collinear, sharing similar stake locations. MTJ105 was 165 meters long with 3-meter spacing to share the same

17

depth of investigation as the previous surveys taken on Field 12. MTJ104 was 55 meters long with 1-meter spacing for a higher resolution of the same area as MTJ105. These two were approximately 40 meters to the north of MTJ12 and both started at the edge of the field nearest the stream. The third transect shared the north-south orientation of transects MTJ08 & MTJ09 and was collected as part of a northern extension to MTJ08. MTJ106 was 165 meters long with 3-meter spacing to share the same depth of investigation as the other surveys on Field 12. These surveys examined the northern edge of the field (the lowest corner of the field), and increased the area of investigation. Locations of the soil samples for the applied sites (Field 12 and 1), samples were collected in both the application zone and the unapplied edge of the field (100 feet from edge of field). The sample locations of Field 12 were denser nearest to the edge of the application zone to try and determine if the boundary between application zone and the unapplied edge of the field can be visualized and paired with the ERI data consistently. The samples correlate to distances along MTJ105 (Figure 7).
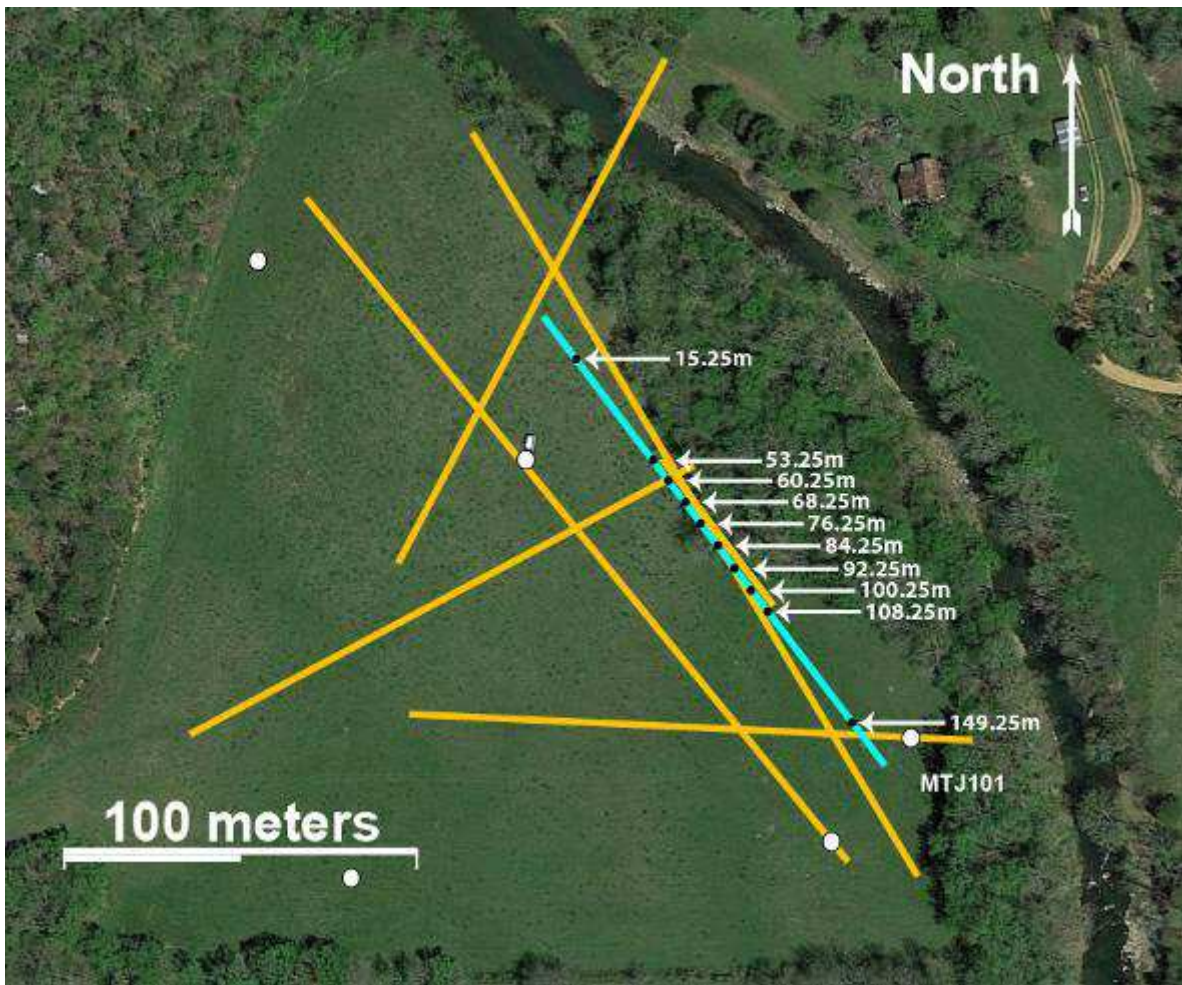
Figure 7 – Black dots represent soil sample locations along transect MTJ105 (blue line) on Field 12 (application site). Yellow lines represent other ERI lines collected at site.

5.2.3 Field 1

In March 2015, two ERI transects (MTJ111 & MTJ112) were collected at Field 1 (Figure 5). The two transects are collinear and are oriented north-south. MTJ111 was 165 meters long with 3-meter spacing so as to share the same depth of investigation as the previous surveys taken on the other fields. MTJ112 was 55 meters long with 1-meter spacing for a higher resolution of the same area as MTJ111. For the applied sites (Field 12 and 1), samples were collected in both the application zone and the unapplied edge of the field (100 feet from edge of field). The sample locations of Field 12 were denser nearest to the edge of the application area to try and determine if the boundary can be visualized and paired with the ERI data consistently. The sample locations of Field 1 were denser in the small gully in the center of the line but also attempted to determine if there is a difference in the application zone and the unapplied edge of the field. The samples correlate to distances along MTJ111 (Figure 8).
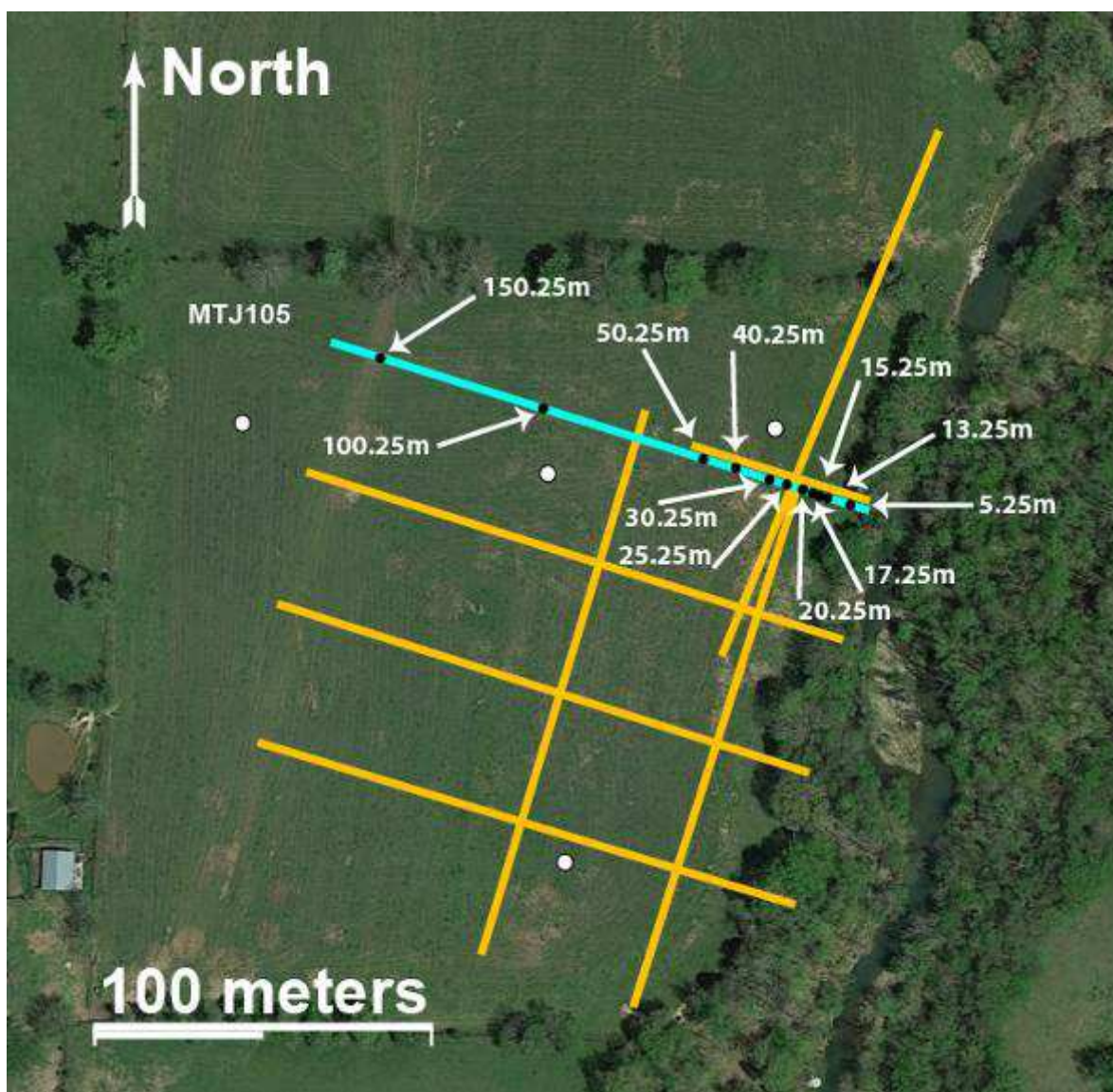
19

Figure 8 – Black dots represent soil sample locations along transect MTJ111 (blue line) on Field 1 (recent application site). Yellow line represent other ERI line collected at site.

5.3 Data Analysis

During previous work to install monitoring wells by the University of Arkansas, soils were hand-augured until hitting a surface hard enough to prevent further penetration (also known as depth of refusal). These depths were evaluated along with the ERI surveys to produce a distributed understanding of the soil depth and thickness across the sites. The epikarst thickness was found using the ERI surveys based on the use of a strong vertical resistivity gradient to delineate weathered epikarst from competent bedrock. Electrically conductive features can be displayed as pathways within the soil and epikarst. Resistive electrical layers are interpreted as the limestone bedrock at depth on each site. Linear electrically conductive pathways through the bedrock are interpreted as potential joints or faults. Electrically conductive zones are interpreted as potential dissolution or weathered portions of the bedrock.

Statistical analysis was run on the ERI data to determine if statistically significant differences existed between the soil ERI data among the three fields. Data were selected from the

20

upper line of each dataset where soil samples were collected. The data were averaged to smooth out variability using a five point moving average. A two-tailed t-test was used to determine significance and alpha was assumed to be 0.05, or the 95% confidence interval. The data were also tested for the three sites to evaluate if the 0.5-meter resolution data were statistically different from the 1.5-meter resolution datasets.

Statistical analysis was run on the soil sample test results to determine if significant variations existed in the parameters between the three fields (see Appendix 6 for data). A two-tailed t-test was used to determine significance and alpha was assumed to be 0.05, or the 95% confidence interval. A margin of error was calculated as $0.98/\sqrt{n}$ (Johnson and Bhattacharyya, 2006), where n is the number of samples. Analyses were performed to compare the background data against the applied sites and to compare the recently applied site to the other two sites.

Correlation between the datasets was analyzed by comparing the two soil types sampled in the background field against the soil analysis data. Correlation for the applied sites was performed by comparing the areas inside the application zone against the corresponding ERI data. Goodness of fit estimates for the relationships were calculated using Excel. The goodness of fit analyses were separated into one of four categories: none or very weak relationship ($r^2 < 0.1$), weak relationship ($0.1 < r^2 < 0.3$), moderate relationship ($0.3 < r^2 < 0.5$), and strong relationship ($0.5 < r^2$).

6.0 Results

Field work in Mt Judea consisted of two trips for a total of eight field days. Lab work for processing and interpreting data constituted months of the project. Results include the processed and corrected GPS data; processed ERI data detailing soil, epikarst, and bedrock features; and soil analysis comparing the soil chemistry and nitrogen isotopes. Resulting raw data can be found in the electronic report appendices.

6.1 GPS Data Analysis

Location data was collected using the GPS system and processed to evaluate the position of the ERI datasets and site topography. The base data were submitted to the Online Positioning User Service (OPUS), operated by the National Oceanic and Atmospheric Administration (NOAA), and the products were corrected for easting, northing, and elevation of the base positions in UTM coordinates. These were applied to the datasets to obtain centimeter-scale accuracy for the topography in the ERI datasets.

6.2 ERI Data Structure

The average root mean square error (RMSE) between the resistivity model and the field apparent resistivity data was 3.16% for Field 5a and 3.34% for Field 12. For Phase II, the processed ERI datasets averaged a RMSE of 3.95% for Field 5a, 3.35% for Field 12, and 6.18% for Field 1. The lower the RMSE percentage, the better the relationship between the collected apparent resistivity data and the calculated subsurface resistivity model. Values above 15% are considered poor. The range of RMSE for the site was 3.0% to 7.8% overall, with an average RMSE of 4.0%. The data quality for the site is good. There were no utilities or other anthropogenic features and the soil was moist at the time of data collection, providing good contact with the ground.

The resistivity values for the sites range from *very electrically conductive* to *highly resistive* (Figure 9). The terms used to indicate a specific range are indicated in *italics* for clarity. Electrically conductive areas generally include the shallow portions of the images, with strong resistors at depth. The resistivities for Field 5a range from 1 to 6×10^5 Ohm-meters with a median value of 1500 Ohm-meters. The resistivities for Field 12 range from 20 to 6×10^5 Ohm-meters with a median value of 1600 Ohm-meters. The resistivities for Field 1 range from 4 to 1×10^6 Ohm-meters with a median value of 1300 Ohm-meters.

The interpretation scale for the resistivity values of the images is electrical features:

- **Above 1000 Ohm-meters** generally represent unweathered bedrock with fresh groundwater and referred to as *highly resistive*.
- **Between 500 to 1000 Ohm-meters** represent weathered bedrock with fresh groundwater and referred to as *very resistive*.
- **Between 150 and 500 Ohm-meters** typically represent significantly weathered bedrock material with fresh groundwater and referred to as *resistive*.
- **Less than 150 Ohm-meters** (but greater than 50 Ohm-meters) are interpreted as soil and/or possible electrically conductive fluids and referred to as *electrically conductive*.

- **Below 50 Ohm-meters** represent fine soils, microbial mass, and/or electrically conductive fluids and referred to as *very electrically conductive*.

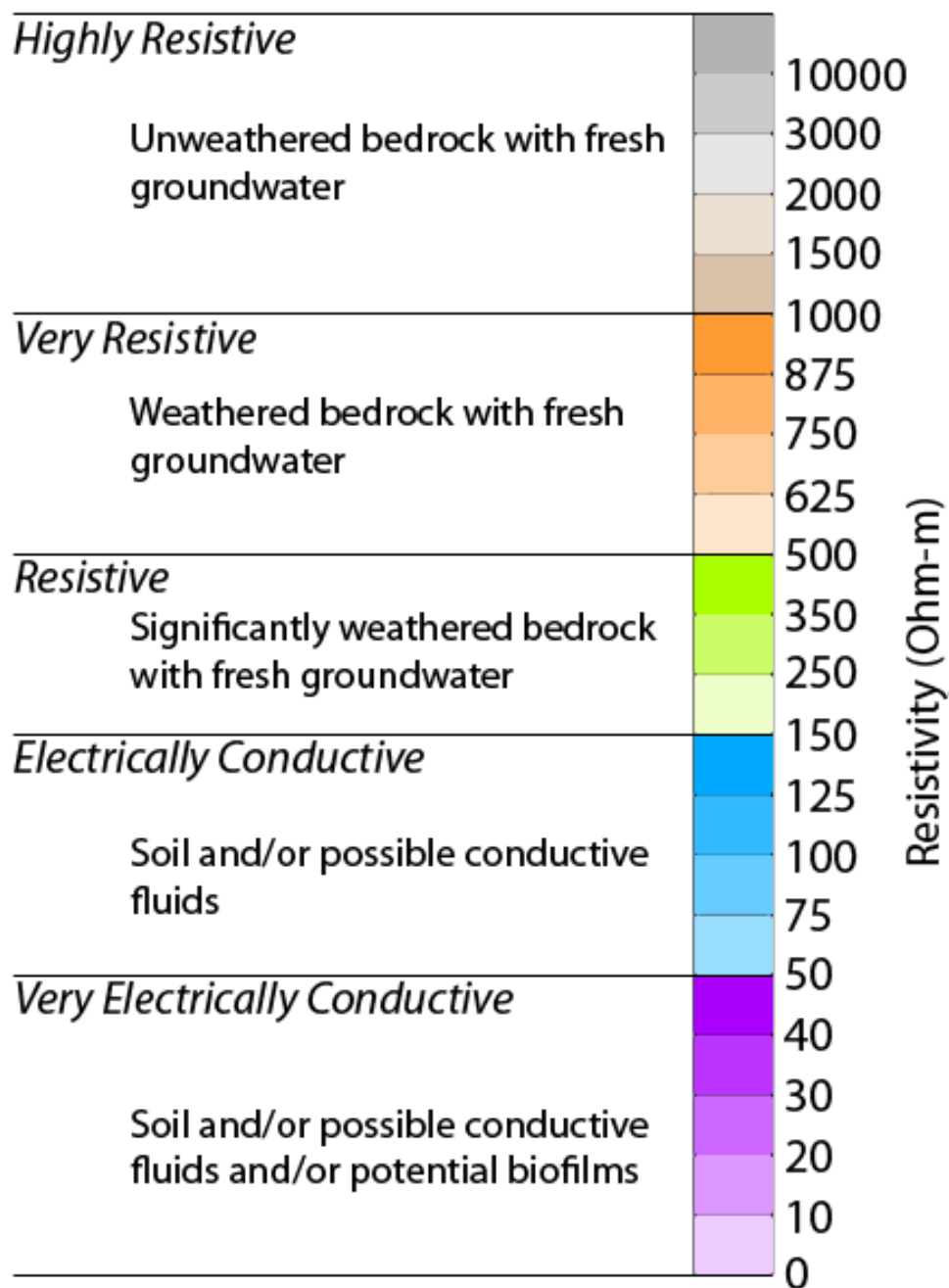*Figure 9 – Resistivity scale for Mount Judea ERI datasets. Cool colors are used to indicate more electrically conductive subsurface locations and warm colors are used to indicate more resistive locations.*
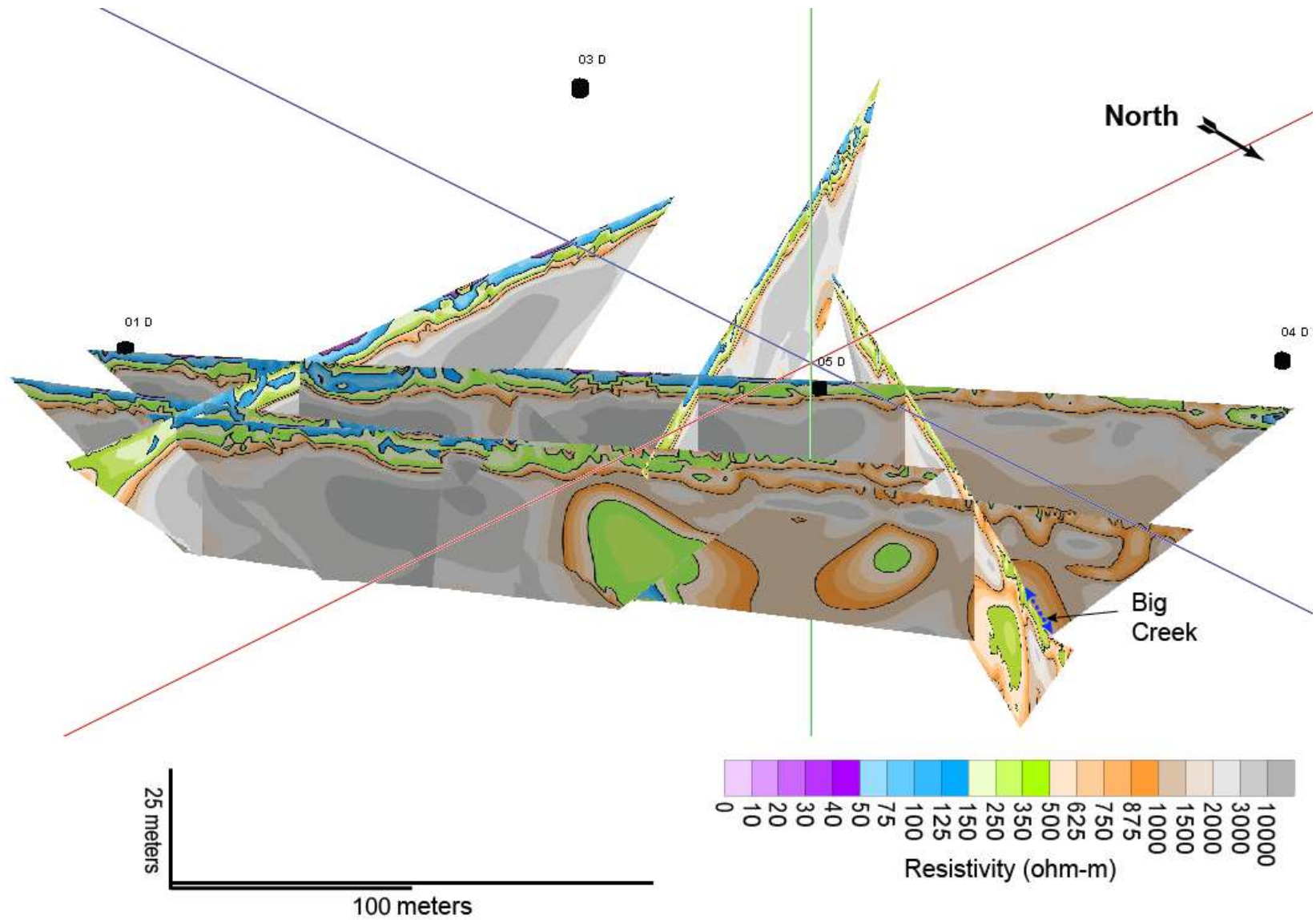
Figure 10 – Field 5a (background site) view from northeast corner of field (from Big Creek toward the field).
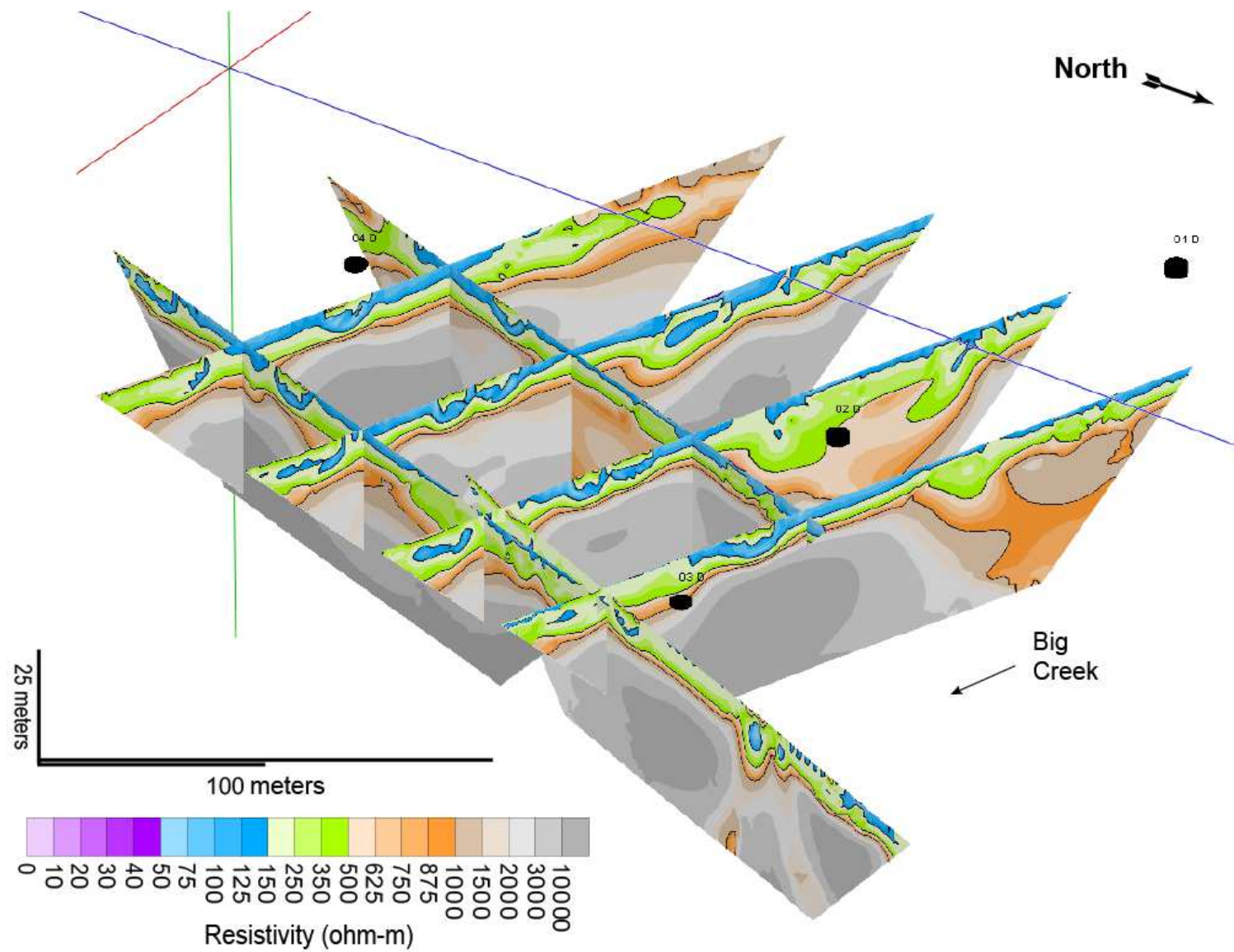
Figure 11 – Field 12 (application site) view from northeast corner of field (from Big Creek toward the field).

6.2.1 Soil Structure

The soil structure analysis consists of soil thickness and soil properties. Soil thicknesses for each site were picked and confirmed through hand dug borings on site conducted during previous University of Arkansas work on these fields. The borings were dug to refusal, or where the soil turns to epikarst (significantly weathered bedrock). Soil properties were detailed based on field notes, ERI results, and grain size analysis.

Field 5a is a low-lying grazing area with low relief and an uneven topsoil surface. Field 5a exhibits average soil thicknesses of 0.5 to 4.5 meters (1.5 to 14.75 feet). Soil thickness on Field 5a varies throughout. There is a significant resistivity difference between the *highly* to *very resistive* north and more *electrically conductive* southern portion (Figure 10). A broad topographic mound is situated northwest of the center of Field 5a; the soil thickness is thinner to the far north and far west of the field (see Appendix 3). This trend is consistent with the direction to which the alluvium would be deposited nearest to the stream. Soils on transects MTJ06 and MTJ07 (Figure 12A) are *electrically conductive* features, which thin to near zero soil thickness toward the far north. Grain size analysis (see Appendix 6) indicates Field 5a is a sandy loam to clay loam. Field 5a and Field 12 share some of the soil characteristics.

Field 12 is a low-lying grazing area with low relief and an uneven topsoil surface. Field 12 exhibits similar average soil thicknesses at 0.7 to 4 meters (2.25 to 13 feet). Soil thickness on Field 12 is not as variable as Field 5a, but there is a *very resistive* region of the site in the shallow soil area of the southwest portion of the investigation area (Figure 11). Field 12 is flatter and the soil thins to the west (see Appendix 3). MTJ12 (Figure 13A) shows thinning where the *electrically conductive* features become thicker as the image gets closer to the stream. This trend is consistent with the direction to which the alluvium would be deposited nearest to the stream. Areas where the soil profile is thinner on the images are consistent with the rocky soils encountered when electrodes were placed for data collection. Grain size analysis (see Appendix 6) indicates Field 12 is a sandy loam to clay loam.

Field 1 is a grazing area situated on a hillside east of the stream. It has low to moderate relative relief and an uneven topsoil surface. Field 1 shows an average soil thickness of 0.5 meters (1.5 feet) determined from the ERI surveys of MTJ111 and MTJ112 (Figure 17) and soil sampling. Hand dug confirmation borings were not conducted on this field. This site was not studied extensively enough to determine differences in resistivity correlations across the entire field. Field 1 has thinner and rockier soils than either Fields 5a or 12. Gravels were found in Field 1 samples with sizes up to 0.05 meters (2 inches) across and subsequently removed during soil sampling. Field 1 has a different soil thickness and properties than Fields 5a or 12.
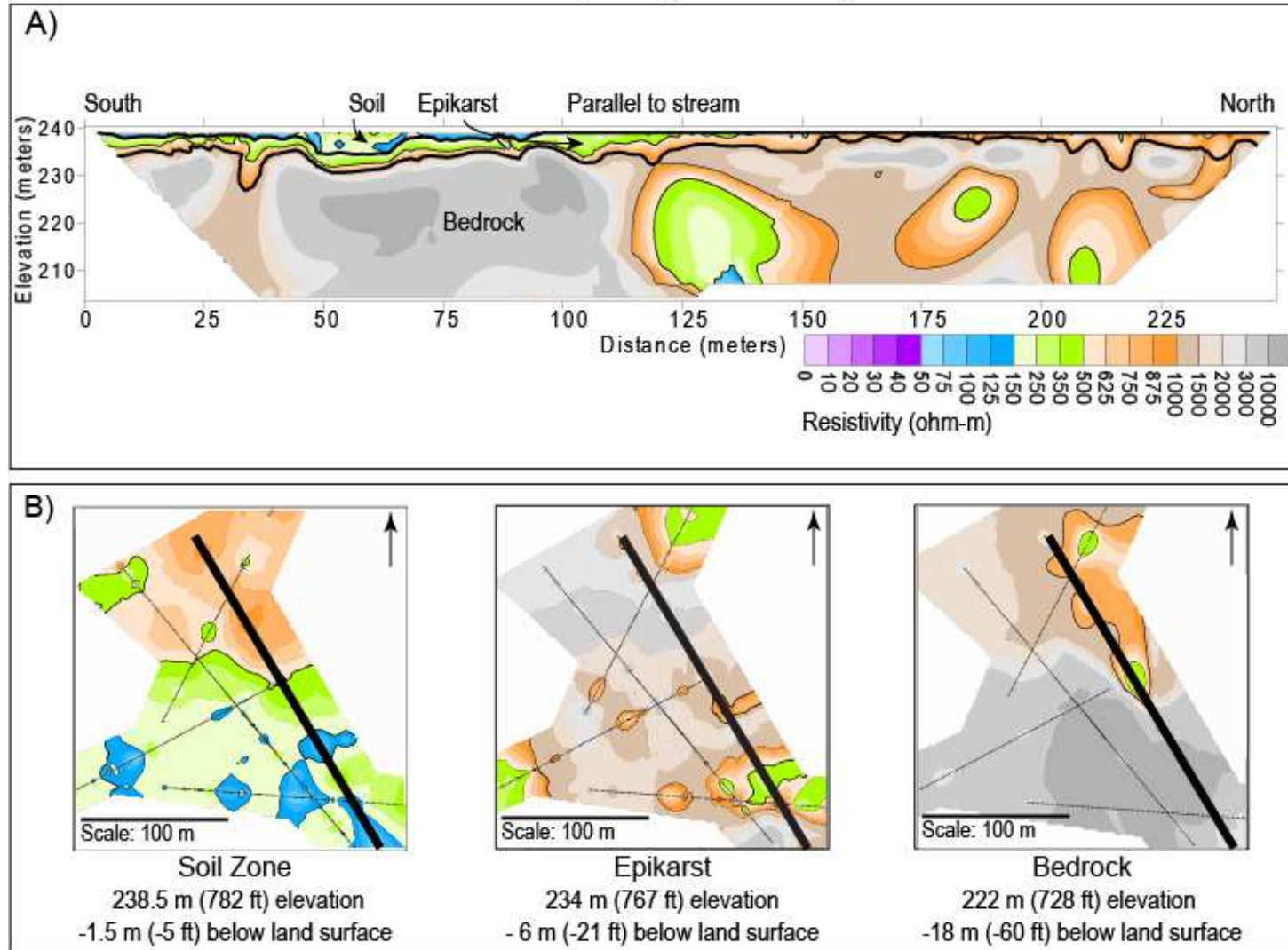
Figure 12 – A) Interpreted Soil-Epikarst boundary and Epikarst-Bedrock boundary for the Field 5a for combined ERI datasets MTJ06 and MTJ07 (background site) cross sections. B) Interpolated 2D depth slices of resistivity at differing elevations illustrating a map view of the subsurface. Heavy black line indicates location of cross section in A).

27
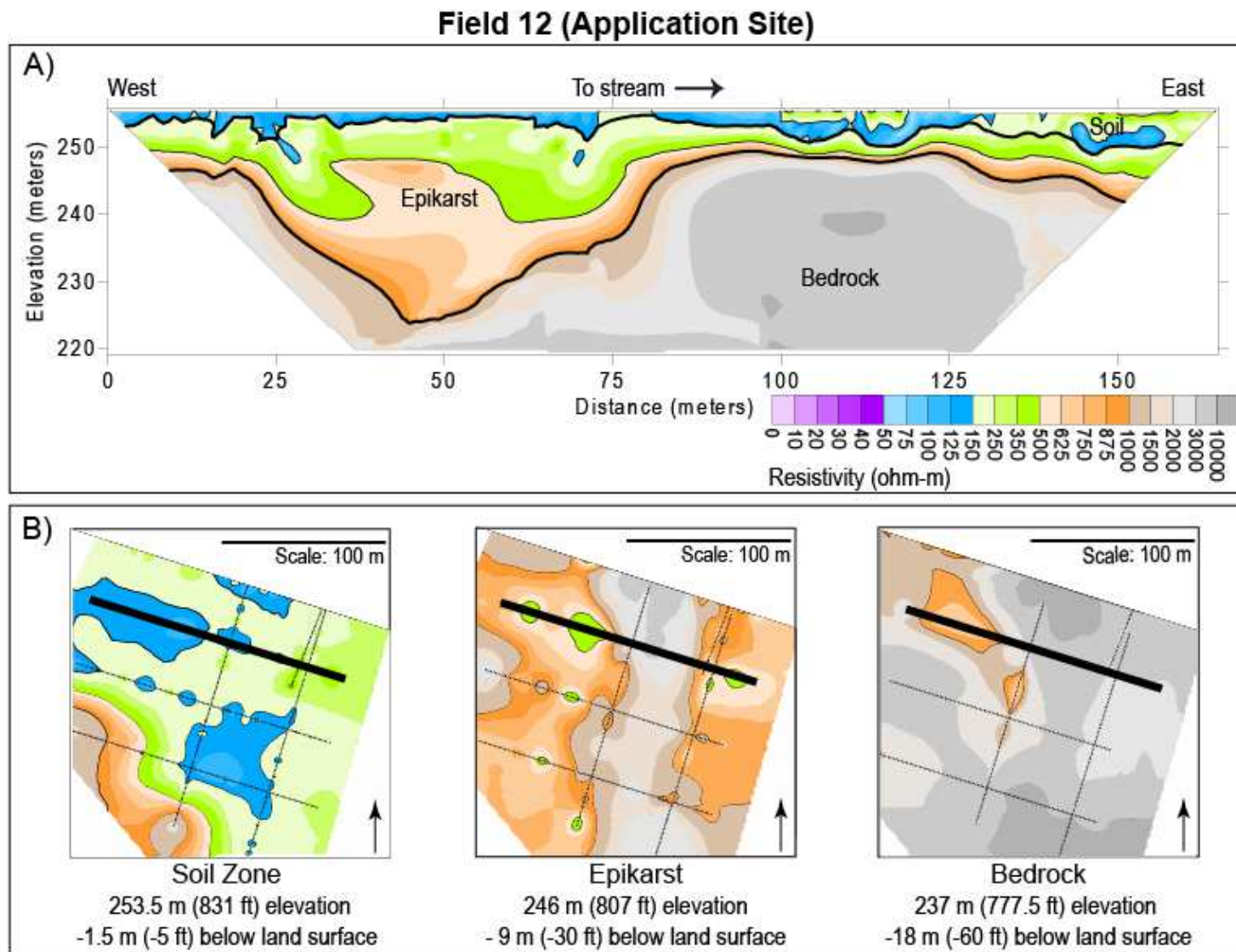
Figure 13 – A) Interpreted Soil-Epikarst boundary and Epikarst-Bedrock boundary for Field 12 for ERI dataset MTJ12 (application site) cross sections. B) Interpolated 2D depth slices of resistivity at differing elevations illustrating a map view of the subsurface. Heavy black line indicates the location of the cross section from A).
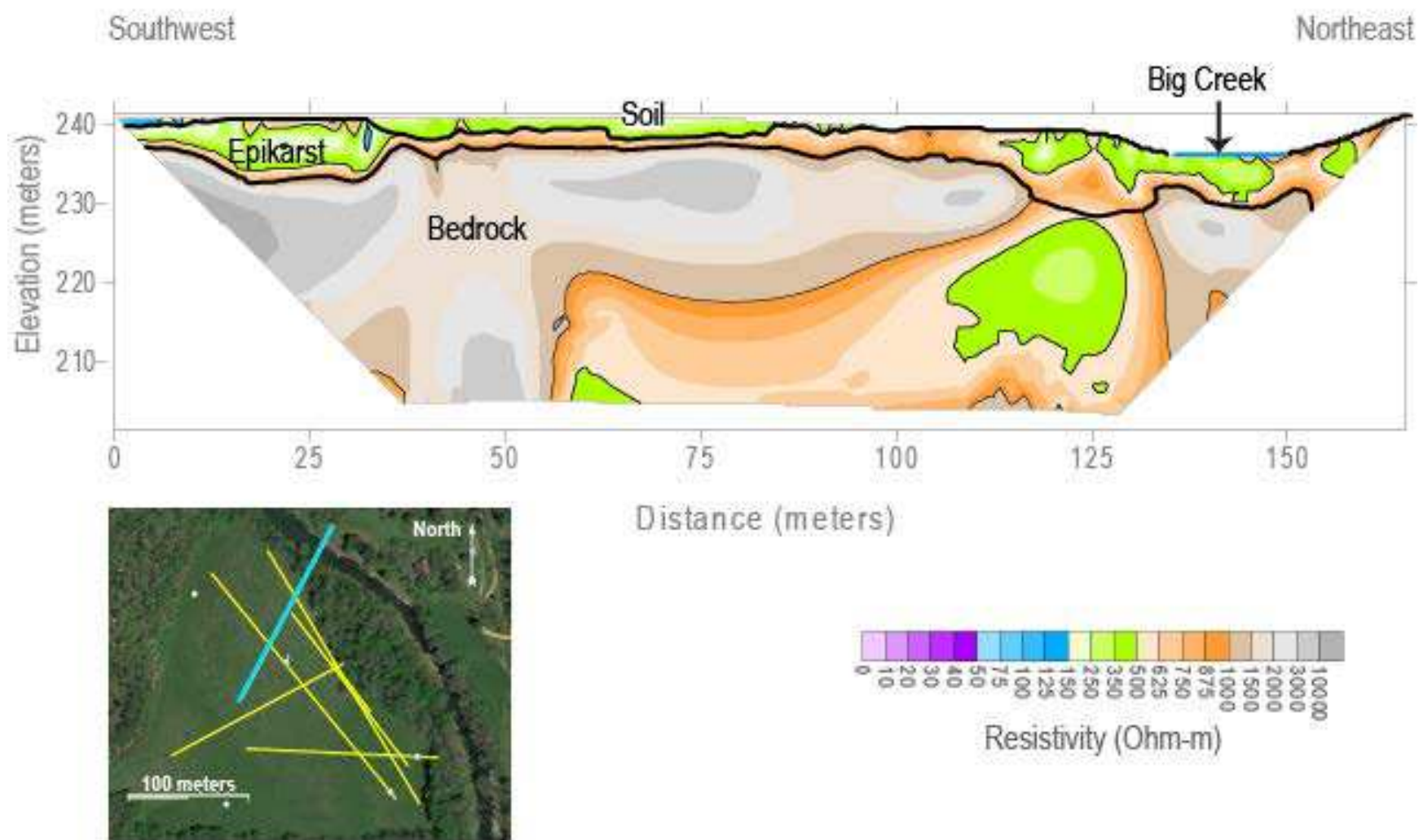
Figure 14 – Field 5a (background site) – Transect MTJ01 with 3-meter spacing.
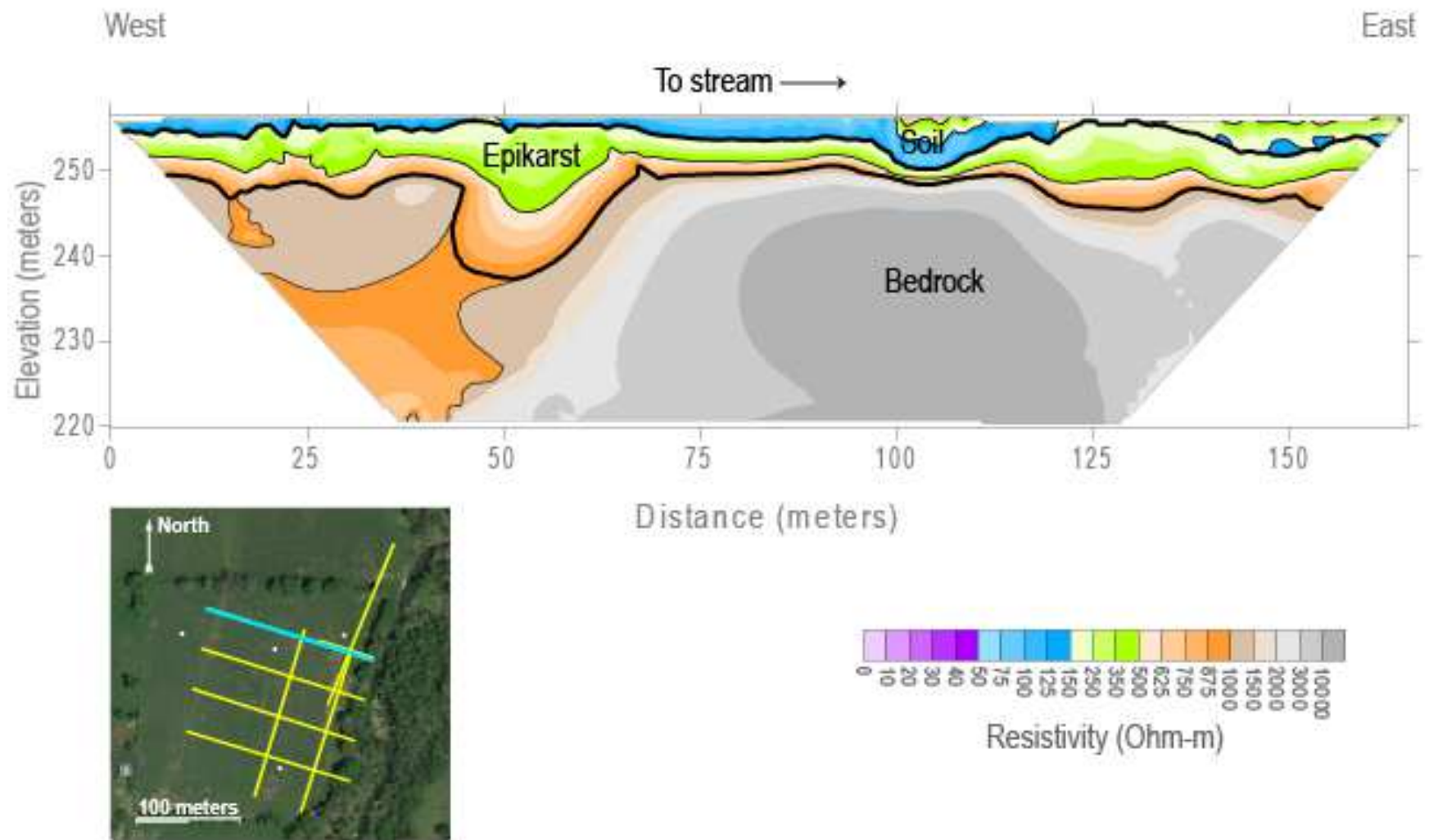
Figure 15 – Field 12 (application site) – Transect MTJ105 with 3-meter spacing.
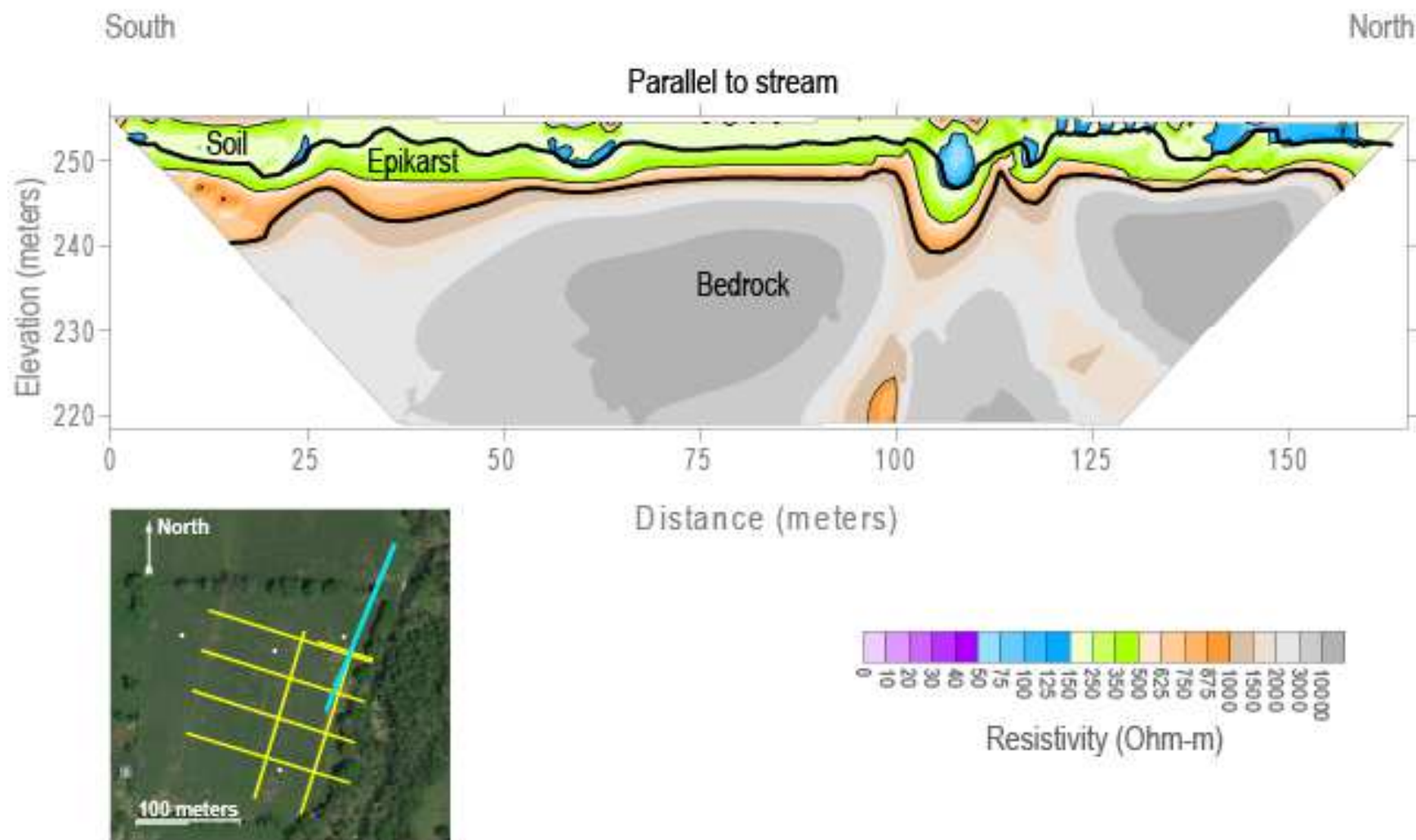
Figure 16 – Field 12 (application site) – Transect MTJ106 with 3-meter spacing.
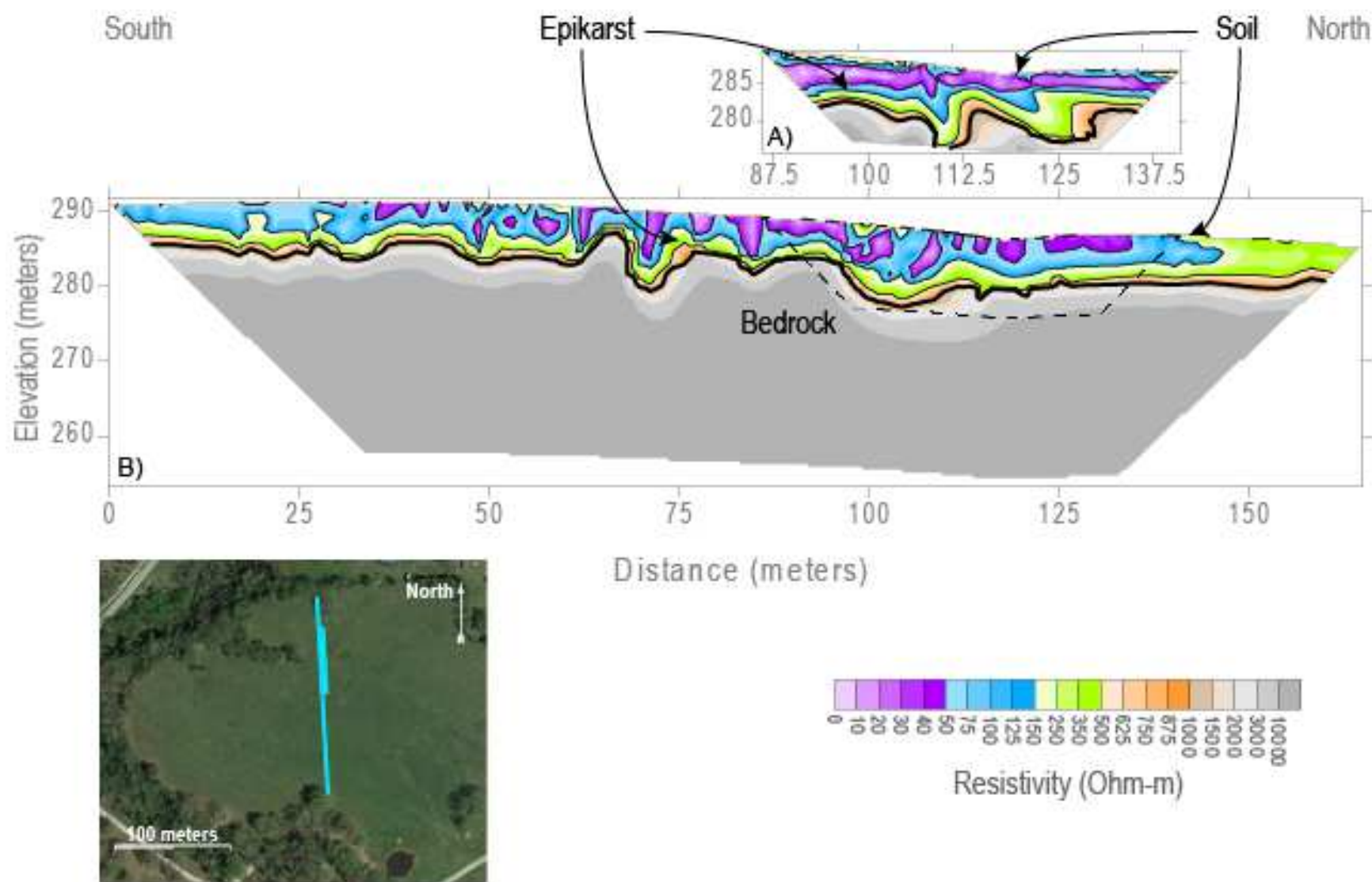
Figure 17 – Field 1 (recent application site) – Transect MTJ111 with 3-meter spacing and Transect MTJ112 with 1-meter spacing.

6.2.2 Epikarst Structure

The epikarst zone consists of the weathering profile of the underlying competent bedrock. Epikarst is visible on Field 5a (Figure 12), Field 12 (Figure 13), and Field 1 (Figure 17) as a more *resistive* to *electrically conductive* region below the base of the soil and above the *highly resistive* competent bedrock zones. No confirmation borings are available to evaluate rock properties in these zones on any of the sites. The thickness of the epikarst zone is highly variable (thicknesses range from 2 to 23 meters or 6.5 to 75.0 feet) throughout each field but averages 4 to 7 meters (13 to 23 feet) thick. Because the interpreted base of the epikarst varies from site to site, the threshold for competent rock was quantified at values larger than 1000 Ohm-meters. This is consistent with a strong horizontal resistivity gradient across the images (Figures 10, 11, and 17).

Average epikarst thickness for Field 5a is 4 meters (13 feet). It is relatively thin and similar to the soil zone, thicker in the southern half of the field. At locations where electrically conductive features exist in the bedrock, the epikarst generally appears connected in space with these features (Figures 12 and 14). ERI dataset MTJ01 shows the most variation in epikarst thickness on Field 5a (Figure 14).

Average epikarst thickness for Field 12 is 6 meters (20 feet) and the epikarst surface on Field 12 is very irregular in many transects (see Appendix 3). There appears to be a large doline feature (a closed topographic depression caused by dissolution or weathering of underlying rock or soil) within the bedrock on transect MTJ12, approximately 61 meters (200 feet) across at the top of the feature, starting 8 meters (26 feet) below the land surface and extending 23 meters (75 feet) vertically downward (Figure 13A).

The determined average epikarst thickness for Field 1 is 5 meters (16.4 feet). Delineating the top of the epikarst from the soil on Field 1 is different from the other sites as there are no hand dug confirmation borings near the transects and the resulting images show *very electrically conductive* features protruding into the subsurface in irregular vertical structures (Figure 17).Most of the samples along the line of soil sampling encountered the top of epikarst with limestone gravel in the top 6 inches of the site. This implies the soil zone is thin relative to the epikarst.

6.2.3 Bedrock

The Boone Formation is the underlying rock unit across these fields and is considered the bedrock. In many of the cross-sections, the limestone is interpreted as large, *highly resistive* blocks. The values for the more competent limestone are interpreted as those greater than 1000 Ohm-meters. It is evident on all three fields (Fields 5a, 12, and 1) that a *highly resistive* zone interpreted as bedrock is located at depth (Figures 12, 13, and 17, respectively). No confirmation borings are available in the bedrock zones to confirm rock properties, but limestone is present in the streams adjacent to Fields 5a and 12, and a quarry is present near Field 1.

Field 5a is, on average, electrically resistive and has a thin layer of alluvium at the foot of a steep hill to the west of the field (Figure 12). The majority of the surveys taken in this field display a very large and blocky *highly resistive* bedrock, especially in the southwest corner. Lines MTJ01 and MTJ06 (Figures 14 and 12, respectively) both show the northern corner of the field is electrically different bedrock than the southern portion of the field (Figure 12B). This zone also has a number of *electrically conductive* features that could be interpreted as karstic zones. The largest of these zones is at 120 meters along ERI line MTJ06/07 (Figure 12A).

Field 12 does not have as many *electrically conductive* features at depth as Field 5a. The field does have some possible doline features within the bedrock (Figure 13A). There are also some possible fractures indicated by vertically oriented conductors to the northern section of the field in MTJ105 and MTJ106 (Figures 15 and 16, respectively). The bedrock here appears more competent and blocky than Field 5a, but still appears to be potentially fractured.

Field 1 does not have the same alluvium layer above limestone bedrock as Field 5a and 12, therefore the bedrock boundary is shallower on this site alone. Field 1 does not share the same fractured characteristics as the other two sites (Figure 17). This site has a very high electrical gradient going from the epikarst zone to the *highly resistant* bedrock.

6.2.4 Site Comparison of ERI Data

A difference can be seen in bulk electrical resistivity values of the three sites. Fields 5a and 12 compare favorably with very similar electrical resistivity values. The resistivities for Field 5a range from 1 to 6×10^5 Ohm-meters with a median value of 1500 Ohm-meters. The resistivities for Field 12 range from 20 to 6×10^5 Ohm-meters with a median value of 1600 Ohm-meters. Field 1 is slightly more electrically conductive overall when comparing the three sites. The resistivities for Field 1 range from 4 to 1×10^6 Ohm-meters with a median value of 1300 Ohm-meters. The values of bulk electrical conductivity (the inverse of electrical resistivity) from the top of the three 165-meter long, 1.5-meter resolution ERI transects, one from each site, run during Phase II, show a difference between the electrical conductivity of Field 1 and the electrical conductivities of Fields 5a and 12 (Figure 18). The increases in Field 1 and Field 12 occur at around 30 meters laterally on the image, which would be the boundary of application of manure. , The strong variations between the fields are not as clear in the higher resolution datasets (55-meter long, 0.5-meter resolution). Field 1 still has the most conductive feature, but it is similar to a feature on Field 5.
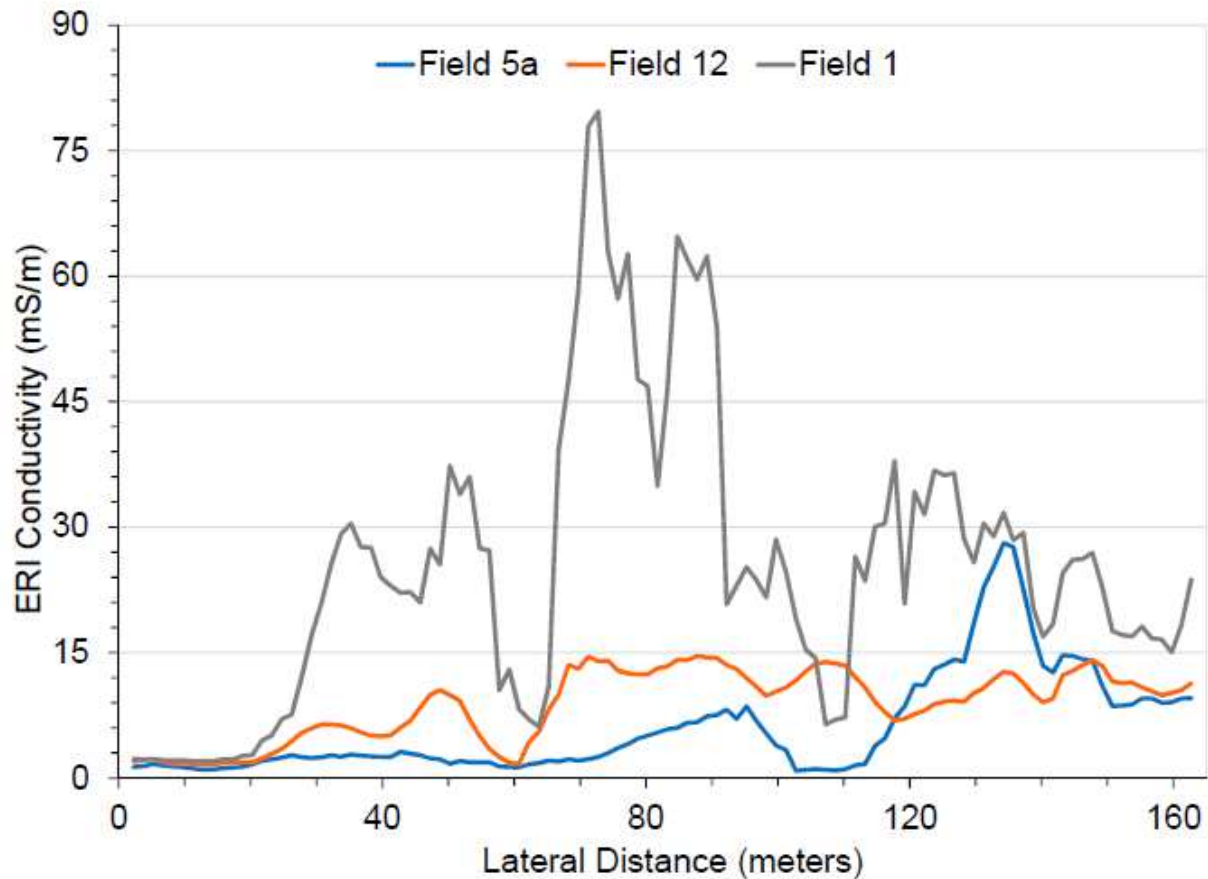
Figure 18 – Electrical conductivity of the top row of data from each site during Phase II at 1.5-meter resolution. Data has been smoothed with a 5 point moving average to make the plot clearer.

6.3 Soil Analysis

Soil samples were collected along the ERI transects during March 2015 to correlate between geophysical (resistivity data) and physical and chemical properties of the soil. In sum, 31 soil samples were collected, across the three fields (see Appendix 6). Statistics were run on the results to determine if there are any correlations between the fields, soil types, or applied versus unapplied areas.

6.3.1 Soil Testing

Soil tests were conducted to examine all three sites. The tests were then compared to determine if there were trends in the data. Soil pH and elements extracted by Mehlich-3 are averaged across all samples collected in each field and given in Table 1 (full dataset given in Appendix 6). Similarly, values for the soil salinity test for each field are averaged and presented in Table 2 (full dataset given in Appendix 6). Fields 1 and 12 (application sites) are consistently higher than Field 5a (i.e., background) in many constituents (Tables 1 and 2). Field 1 is highest in all categories except in calcium and sodium values. Field 1 has similar values to Field 12 in both fluid electrical conductivity (EC) and total soluble salts (TSS). Statistical analysis was conducted to determine of there were significant differences among sites.

35

Table 1 – Soil sampling averages for various constituents on each field after Mehlich-3 extraction method (dry method for solids analysis).

Constituents	Field 1	Field 5a	Field 12
pH	6.5	5.4	5.7
P (ppm)	83.2	49.3	72.1
K (ppm)	232.1	66.5	100.9
Ca (ppm)	1314.8	1283.0	1696.9
Na (ppm)	15.4	15.1	107.6
Mg (ppm)	129.2	76.7	13.9
SO_4 (ppm)	28.6	24.5	28.7
Fe (ppm)	194.6	170.4	179.0
Mn (ppm)	636.4	188.7	201.1
Cu (ppm)	1.6	1.4	1.9
Zn (ppm)	5.0	2.6	4.3
B (ppm)	0.1	0.1	0.1

6.3.2 Nitrogen Isotopes

Isotope analysis was conducted and compared for trends in the data to examine all three sites. Nitrogen isotope analysis was utilized to determine if there was a detectable signature of the applied hog manure within any of the soil samples. The del 15N/14N ratio ($\delta^{15}N / \delta^{14}N$) is compared to isotope signatures from other agricultural areas. The data from all 31 samples and their duplicates ranged from 3.803‰ – 6.628‰ across all three sites. The average is lowest for Field 1 (recent application site), with an average at 4.762‰ (0.485 SD) and a range of values from 3.944‰ – 5.811‰. Field 5a (background site) has the next larger average $\delta^{15}N / \delta^{14}N$ ratio with a value of 5.101‰ (0.606 SD) and a range of 3.803‰ – 6.314‰. Field 12 (application site) has the largest average ratio at 5.629‰ (0.703 SD) with a range from 4.174‰ – 6.628‰.

Table 2 – Soil sampling averages for various constituents on each field after 1:1 soil-water extraction method (fluid method).

Constituents	Field 1	Field 5a	Field 12
pH	6.7	5.8	6.0
K (ppm)	75.0	6.0	20.7
Ca (ppm)	50.9	38.2	73.5
Na (ppm)	15.2	11.2	12.5
Mg (ppm)	7.4	3.3	6.7
EC (micromhos/cm)	857.9	488.1	891.9
TSS (ppm)	566.2	322.2	588.6
PAR (ratio)	1.6	0.2	0.4
SAR (ratio)	0.6	0.5	0.4
EPP (%)	16.5	5.0	6.9
ESP (%)	0.0	0.0	0.0

6.3.3 Statistical Analysis of Soil Data

In Field 5a (background site), a simple random sample at a 95% confidence interval and a margin of error of 31% was calculated, where *n* is the 10 total samples. This dataset provides an understanding of the relationship among the variables, but it is not statistically strong because the number of samples is small. The constituents (from both Mehlich-3 and 1:1 soil-water methods) of statistical significance were: pH, Ca, Mg, SO_4, Fe, Cu, Zn, B, and EC. The statistical tests were applied to the two halves of the field, divided by soil type. The statistical analysis indicates a significant difference between the northern and southern parts of the field. This is also apparent in the percentage of sand making up soil texture, with the northern portion of the field having a sandier soil.

Figure 19 – Soil sampling results plotted showing the constituents of Field 5a were found to be statistically different from the other fields.

In Field 12 (application site) 11 total samples were analyzed. This dataset provides an understanding of the relationship between the variables, but it is not statistically strong because of the small number of samples. The constituents (from both Mehlich-3 and 1:1 soil-water methods) of interest were: pH, P, K, Ca, Mg, SO_4, Cu, Zn, B, EC, and $\delta15N$ / $\delta14N$. The statistical tests were applied to the two groups of soil samples from the field, the unapplied edge of the field and application zone. The statistical analysis indicates there is not a significant difference between the unapplied edge of the field and application zone. Weak and strong relationships between the constituents and the corresponding resistivity values existed.

In Field 1 (recent application site), 10 total samples were available. The statistical tests could not be applied to the two groups from Field 1 because there is only one sample in the unapplied edge of the field and is insufficient for analysis.
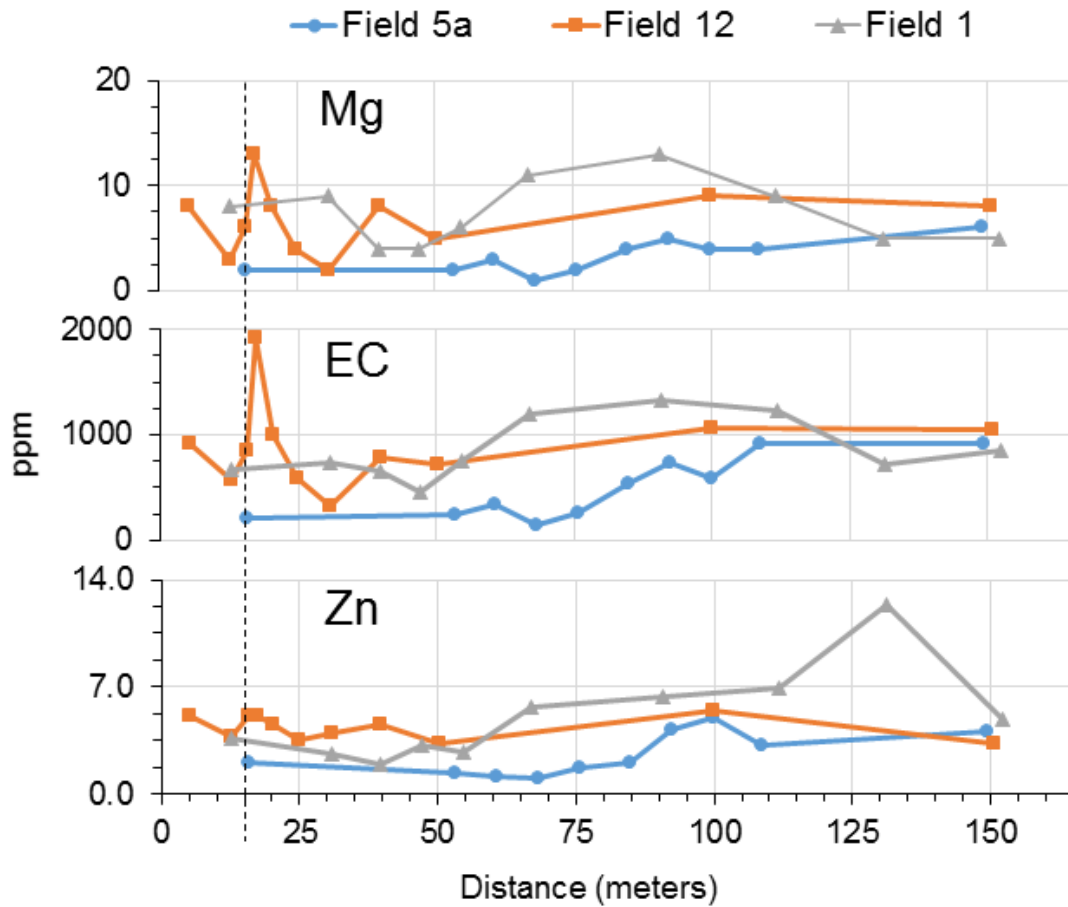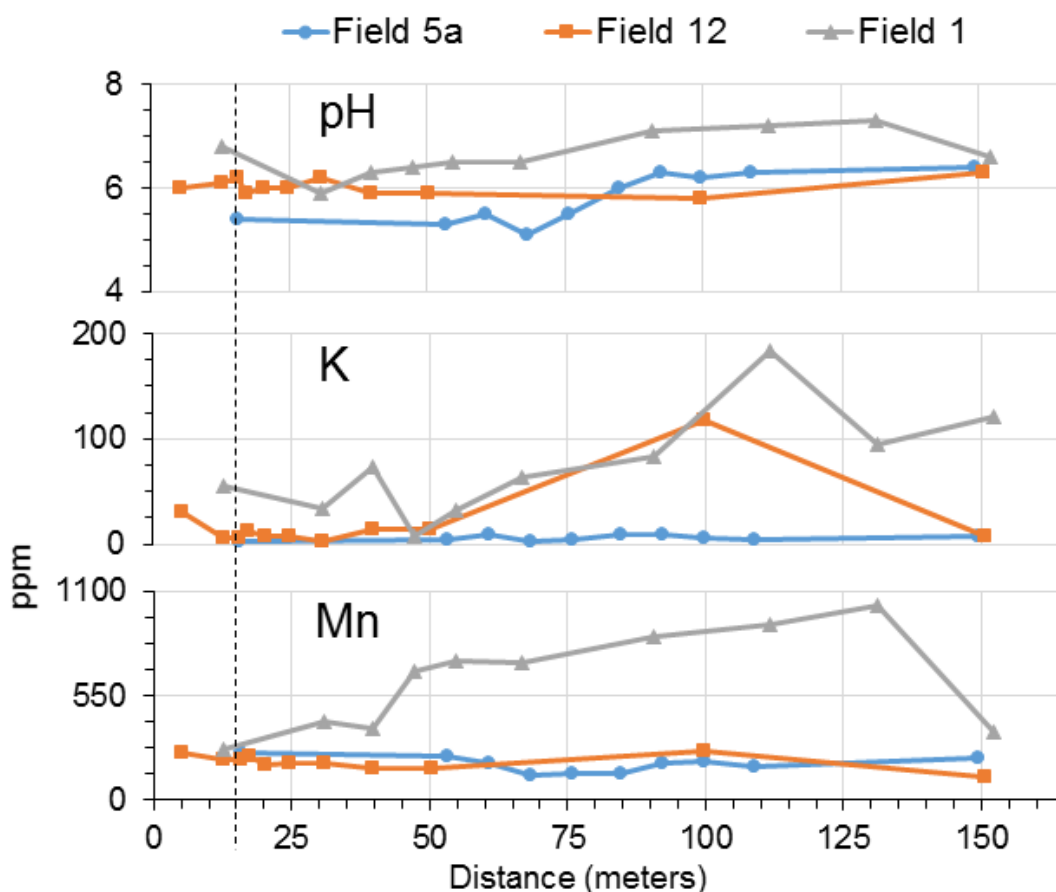
Figure 20 – Soil sampling results plotted showing the constituents of Field 1 were found to be statistically different from the other fields.

The same t-test was run to statistically compare the fields against each other, and compared the constituent of each field. Field 5a is statistically lower than both Fields 12 and 1 in Mg, Zn, and EC. Field 1 is statistically higher than both Fields 5a and 12 in pH, K, and Mn. Although Field 12 was statistically different in some constituents for one field, it was not statistically different for the other field.

Isotopic signatures were used to find the isotopic signature of hog manure. Finding, or not finding, a particular isotopic value indicates whether or not the soil samples contained any trace amounts of hog manure. The $\delta15N$ / $\delta14N$ values ranged from 3.803 ‰ to 6.628 ‰ across all three fields. Field 5a had higher average values than Field 1. When comparing this to a compilation of other data, we see this range falls on the peaks of "natural" and "fertilized" soils, and in fact are at the low end for "animal waste" values (Aly et. al, 1981; Aravena et. al, 1993; Black and Waring, 1977; Bremner and Tabatabai, 1973; Fogg et. al, 1998; Freyer, 1978, 1991; Garten, 1992, 1996; Gormly and Spalding, 1979; Heaton, 1986, 1987; Heaton et. al, 1997; Hoering, 1957; Kohl et. al, 1971; Kreitler, 1975, 1979; Moore, 1977; Paerl and Fogel, 1994; Shearer et. al, 1974, 1978; Wolterink et. al, 1979). Hog waste $\delta15N$ / $\delta14N$ averages have been found to be within 10 ‰ to 20 ‰ range (Fogg et. al, 1998; Krietler, 1975, 1979; Wolterink et. al, 1979). The fields do not provide a significant N isotopic signature in this dataset to allow for the

separation of signatures for applied manure and other sources of N (i.e., native, fertilizer, poultry litter).

6.3.4 Site Comparison

Field 5a shows a distinct trend in bulk electrical resistivity data which compares well with soil thickness and soil test results. The electrical resistivity data in Figure 18 shows a much more resistive half of the field in the north (0 – 80 meters) and a more electrically conductive half of the field in the south (80 – 165 meters). To the north, the site thins to a rocky soil; to the south it thickens and the soil is composed of finer particles. Figure 19 shows the soil test results for this site and indicate the north half of the field has lower values for the three *distinctly different* constituents: Mg, Zn, and electrical conductance.

Field 12 appears to have somewhat more electrically conductive soil over a broader area than Field 5a and shows an overall increase in bulk electrical conductivity from 30 meters (100 feet). This electrically conductive area is not located near the stream, where application of manure would not occur (unapplied edge of the field) under the recommended protocols of the comprehensive nutrient management plan. The electrical resistivity data shows consistency across the entire field. The soil thickness is also thicker across the entire field when compared to Field 5a. Soil test results showed no indication Field 12 was statistically different from the other two fields.

Field 1 does not share the same electrical features seen in the alluvium of Fields 5a and 12, but does appear to have more electrically conductive features present within the epikarst zone. The features present show a relatively more resistive soil zone but a *very electrically conductive* epikarst zone that extends nearly the length of the field and dissipates at the unapplied edge of the field, approximately 30 meters (100 feet) from the northern edge of the field. This distance from the northern edge of the field is consistent with the recommended protocols of the comprehensive nutrient management plan for where the application of manure would not occur. The soil on this site was thin and rocky and grain size analysis showed this site was different than the other two sites. Figure 20 shows the soil test results for this site and indicate three *distinctly different* constituents are higher than the other two sites.

The anticipated ERI relationship with fluid electrical conductivity of soil water samples would be as electrical conductivity of the fluid increased, the bulk resistivity of the soil would decrease. There was no strong relationship between these parameters for the lower resolution (1.5-meter) datasets. While these datasets showed the applied fields had a higher bulk conductivity (lower resistivity) than the background sites, the datasets averaged too deeply into the subsurface, leading to some significant contrasts at the surface between the two ERI dataset resolutions.

The expected the relationship held for the background site (Field 5a) for the higher resolution dataset (Figure 21). The fluid EC has an inverse relationship with bulk resistivity with an R^2 value of 0.56. The applied fields have an inverse relationship with higher EC fluids resulting in higher resistivity zones with an R^2 value of 0.50 for Field 12 and 0.98 for Field 1. This type of relationship indicates the bulk electrical properties are not only responding to the addition of a fluid with a higher electrical conductivity, but another soil electrical property must be changing as well. This may be due to the growth of biofilms, as microbial activity increases after the application of manure.
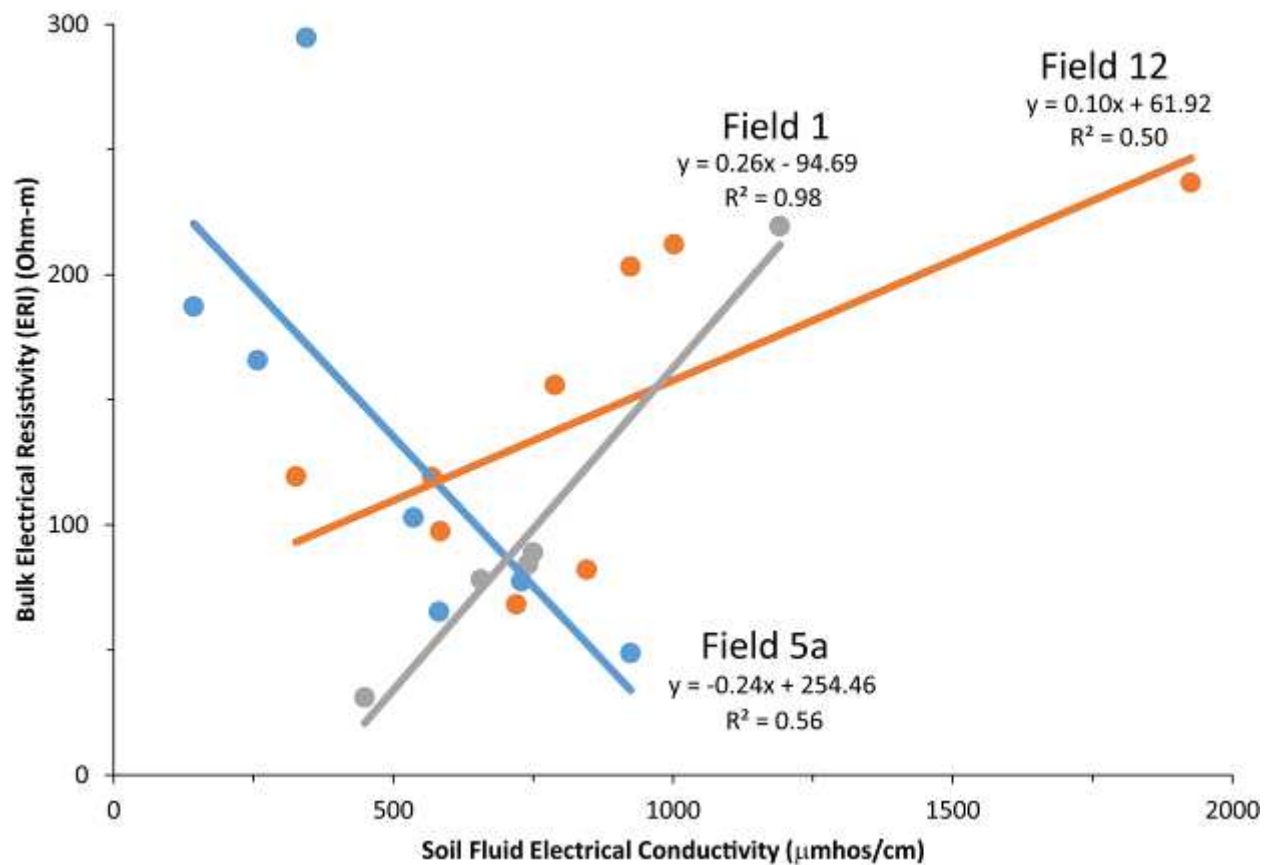
Figure 21 – Soil Fluid Electrical Conductivity measured from soil samples collected along three ERI transects compared with ERI bulk resistivity data with 0.5-meter resolution for three fields near Mount Judea, Arkansas. Field 5a is the background site and Fields 1 and 12 had applied hog manure.

7.0 Discussion

Fields 5a and 12 share many electrical and soil-depth characteristics but there are a few distinctions that separate them from each other. Field 1 is different from the other two sites in many aspects. Soil analysis is a complex issue that requires an in depth investigation to determine possible correlations between constituent levels. Much of the literature points to the overarching idea that individual site testing is required for understanding the individual site's properties. A significant portion of the literature is dedicated to analysis of constituents related to crop growth, but for this work, only constituents that had statistical variations between sites were analyzed.

The electrical structure of the soil, epikarst, and bedrock were consistent with the literature of weathered mantled carbonate bedrock areas (Carriere et al., 2013; Gambetta et al., 2009; Halihan et al., 2005, 2009; Miller et al., 2014; Stepisnik and Mihevc, 2008). The soil thickness increasing towards the streams would be expected in an alluvial valley. The epikarst zone having significant variability in lateral and vertical properties was consistent with evaluations from other carbonate locations (Gambetta et al., 2009; Halihan et al., 2005, 2009). The data are consistent with previous investigations and indicate more permeable flowpaths would exist in the bedrock of the site, but no drilling or hydraulic testing data are available from the sites included in this investigation.

The results of the soil tests are representative of the conditions on each field, but are a small dataset for the fields overall. The sampling was used to evaluate parameters which may change with electrical properties and provide future indicator parameters for geophysical soil monitoring. The concentrations of constituents for Fields 12 and 1 were not sufficiently high to definitively indicate the presence of hog manure when compared to literature values for applied sites (Choudhary et. al, 1996; DeRouchey et. al, 1999; Hannan, 2011; Klimek, 2012; Plaza et. al, 2004; Smith et. al, 2007; Suhadolc et. al, 2004; Turner et. al, 2010). This is expected as the largest amount of application was less than a half centimeter. It is known that constituent levels tend to increase over time as fertilizers are applied depending on the rate of application and rate of crop offtake (Choudhary et. al, 1996; Hannan, 2011; Reddy, 1980; Schoenau, 2006) and it "may take several years of application before significant differences can be detected" (Schoenau, 2006). Currently, the data do show Fields 12 and 1 have consistently higher values for many of the constituents than Field 5a. Vegetation requirements govern application amounts for hog manure to prevent any excess buildup of particular constituents (Racz and Fitzgerald, 2000).

Field 5a was statistically lower in Zn in the soil solids (Table 1), and lower in Mg and electrical conductance in the soil fluid (Table 2) than the other two fields. Studies show Mg levels in soils can be higher due to natural causes from the weathering of limestone (Hannan, 2011; Plaza et. al, 2004) or anthropogenic impacts, such as hog manure (Schoenau, 2006). Field 5a sits primarily on alluvium and does not receive hog manure, which is in the same geologic setting. Lower levels of zinc on the background site is consistent with the literature, as hog manure can carry increased levels of Zn (Klimek, 2012; Racz and Fitzgerald, 2000; Suhadolc et. al, 2004). Lower fluid EC on the background site is consistent with the hog manure soil amendments having higher fluid electrical conductivity (which is physically different than bulk electrical conductivity measured with ERI) (Turner et. al, 2010).

Field 1 was statistically higher in pH, K, and Mn in the soil solids (Table 1) than the other two fields. Field 1 was also statistically higher in pH and K in the soil fluids (Table 2). Fields receiving manure from hogs receiving some types of feed can alter levels of K (Hannan, 2011),

but this can also result from materials weathering from carbonates (Schoenau, 2006). Some fields where the soil is developed from a limestone layer beneath it can have higher pH levels compared to the background site with alluvium soil (Plaza et. al, 2004). A study on the relation of Mn with applied hog manure was not found.

The relationships for the three fields between bulk electrical resistivity and fluid electrical conductivity indicated the relationship to the application of manure did not simply cause the media to become more conductive. Research in biogeophysics indicates microbial activity may be generating the decrease in bulk conductivity (increase in bulk resistivity) as the fluid electrical conductivity increases. If microbial populations are developing to consume the available applied material, this type of relationship between the bulk and fluid properties may occur. Additional research on the microbial populations in the field and transient monitoring of electrical properties would be required for this to be conclusive.

8.0 Conclusions

The field data collected in Mount Judea, Arkansas, in December 2014 and March 2015 characterizes the subsurface of Fields 5a (background site), 12 (application site), and 1 (recent application site) with 1.5-meter resolution on scales of 165 meters laterally and 33 meters vertically. Three additional surveys with 0.5-meter resolution were also conducted to evaluate soil properties with higher resolution. These results were useful in defining the characteristics of the soil zone, epikarst zone, and the bedrock.

8.1 Soil Structure

This series of ERI surveys contributed to understanding the structure and distribution of material underlying Fields 5a, 12, and 1. The surveys confirmed the soil thickness, presence, extent, and depth of epikarst features and bedrock material. The average soil thickness across the sites is very similar (1 to 4.5 meters or 3 to 14.75 feet) except for the area in which Field 5a exhibits thinning of the soil (to 0.5 meters or 1.5 feet). Field 1 had a soil thickness of 0.5 meters (1.5 feet).

8.2 Epikarst Structure

The 33-meter (108 feet) depth of investigation for this experiment was sufficient in finding the vertical electrical changes to high resistivity that are interpreted as the bottom of the epikarst zone. The epikarst thickness is similar on both Fields 5a and 12 with a range of 2 to 23 meters thick (6.5 to 75 feet), with an average of approximately 7 meters (23 feet), but the distribution of possible fracturing in bedrock or karst features was variable, as expected. There is no confirmation drilling at the sites to evaluate rock properties of the epikarst zone, but results are consistent with other investigations of epikarst zones (Williams, 2008). The surveys were consistent among orthogonal lines across the sites in depicting the extent of bedrock weathering and amount of weathering at each site.

8.3 Bedrock

The ERI surveys show the bedrock as consistent, *highly resistive* features. Lateral variations in resistivity values of the bedrock potentially indicate depositional setting of beds or channels and deformation such as faulting. The ERI surveys determined depth to bedrock and highlights possible dissolution features and fracturing typical of this geologic formation.

8.4 Soil Analysis

Soil sampling showed that there are differences among sites. Field 5a's results draw good comparisons between the soil structure and soil tests and has consistently lower values in many of the soil parameters but is only statistically lower in Mg, Zn, and fluid electrical conductance. Field 12 is not statistically different from either site but is still higher than Field 5a in many test results. Field 1 has consistently higher values in many of the soil parameters but is only statistically higher in pH, K, and Mn. These results show statistical differences can be observed in recently applied areas. With lower amounts of application or over time, these signatures may not be detectable.

9.0 References

Allaby, M., eds., 2008, A dictionary of earth sciences: Oxford University Press, Oxford Reference.

Aly, A.I.M., Mohamed, M.A., and Hallaba, E., 1981, Mass spectrometric determination of the nitrogen-15 content of different Egyptian fertilizers *in* Journal of Radioanalytical Chemistry, 67(1), 55-60 p.

Anderson, M.S., 1960, History and developments of soil testing *in* Agricultural and Food Chemistry, 8(2), 84-87 p.

Aravena, R., Evans, M.L., and Cherry, J.A., 1993, Stable isotopes of oxygen and nitrogen in source identification on nitrate from septic systems *in* Ground Water, 31(2), 180-186 p.

Black, A.S. and Waring, S.A., 1977, The natural abundance of 15N in the soil-water system of a small catchment area *in* Australian Journal of Soil Research, 15, 51-57 p.

Bolyard, S.E., 2007, Migration of landfill contaminants in a tilted-block mantled-karst setting in northwestern Arkansas, University of Arkansas, M.Sc. thesis, 69p.

Bremner, J.M. and Tabatabai, M.A., 1973, Nitrogen-15 enrichment of soils and soil-derived nitrate *in* Journal of Environmental Quality, 2(3), 363-365 p.

Carrière, S.D., Chalikakis, K., Sénéchal, G., Danquigny, C., and Emblanch, C., 2013, Combining electrical resistivity tomography and ground penetrating radar to study geological structuring of karst unsaturated zone *in* Journal of Applied Geophysics, 94, 31-41 p.

Chandler, A.K. and Ausbrooks, S. M., revised 2015, Geologic map of the Mt. Judea quadrangle, Newton County, Arkansas: Arkansas Geologic Survey Digital Map, DGM-AR-00590, 1:24,000.

Choudhary, M., Bailey, L.D., and Grant, C.A., 1996, Review of the use of swine manure in crop production: effects on yield and composting and on soil and water quality *in* Waste Management & Research, 14, 581-595 p.

DeGroot, P. A., 2004, Handbook of stable isotope analytical techniques Volume 1, Amsterdam: Elsevier, Print.

DeRouchey, J.D., Keeler, G.L., Goodband, R.D., Nelssen, J.L., Tokach, M.D., and Dritz, S.S., 1999, Manure composition from Kansas swine lagoons *from* Swine Day 1999, 3 p.

Field, M.S., 2002, A lexicon of cave and karst terminology with special reference to environmental karst hydrology: Washington, D.C., United States Environmental Protection Agency, 214p.

Ferguson, J.G., 1920, Outlines of the geology, soils and minerals of the state of Arkansas: Little Rock, State Bureau of Mines, Manufactures and Agriculture, 182p.

Fogg, G.E., Rolston, D.E., Decker, D.L., Louie, D.T., and Grismer, M.E., 1998, Spatial variation in nitrogen isotope values beneath nitrate contamination sources *in* Ground Water, 36(3), 418-426 p.

Freyer, H.D., 1978, Seasonal trends of NH4+ and NO3- nitrogen isotope composition in rain collected at Julich, Germany *in* Tellus, 30, 83-92 p.

Freyer, H.D., 1991, Seasonal variation of 15N/14N ratios in atmospheric nitrate species *in* Tellus, 43B, 30-44 p.

Galloway, J.M., 2004, Hydrogeologic characteristics of four public drinking-water supply springs in northern Arkansas: U.S. Geological Survey Water-Supply Paper 03-4307, 68p.

Gambetta, M., Armadillo, E., Carmisciano, C., Stefanelli, P., Cocchi, L., and Tontini, F.C., 2009, Determining geophysical properties of a near-surface cave through integrated microgravity vertical gradient and electrical resistivity tomography measurements *in* Journal of Cave and Karst Studies, 73(1), 11-15 p.

Garten, C.T., Jr., 1992, Nitrogen isotope composition of ammonium and nitrate in bulk precipitation and forest throughfall *in* International Journal of Environmental Analytical Chemistry, 47, 33-45 p.

Garten, C.T., Jr., 1996, Stable nitrogen isotope ratios in wet and dry nitrate depostion collected with an artficial tree *in* Tellus, 48B, 60-64 p.

Gary, M.O., Halihan, T., and Sharp, J.M. Jr., 2009, Detection of sub-travertine lakes using electrical resistivity imaging, Sistema Zacatón, Mexico *in* paper presented at the 15th International Congress of Speleology, Kerrville, TX., 2009, Proceedings: Kerrville, TX., International Congress of Speleology, Volume 1, 618 p.

Gormly, J.R. and Spalding, R.F., 1979, Sources and concentrations of nitrate-nitrogen in ground water of the Central Platte Region, Nebraska *in* Ground Water, 17(3), 291-301 p.

Halihan, T., Love, A., and Sharp Jr., J.M., 2005, Identifying connections in a fractured rock aquifer using ADFTs *in* Ground Water, 43(3), 327-335 p.

Halihan, T., Puckette, J., Sample, M., and Riley, M., 2009. Electrical resistivity imaging of the Arbuckle-Simpson Aquifer: final report submitted to the Oklahoma Water Resources Board, 92 p.

Hannan, J.M., 2011, Potassium-magnesium antagonism in high magnesium vineyard soils, Iowa State University, M.Sc. thesis, 40 p.

Heaton, T.H.E., 1986, Isotopic studies of nitrogen pollution in the hydrosphere and atmosphere: a review *in* Chemical Geology (Isotope Gesciences Section), 59, 87-102 p.

Heaton, T.H.E., 1987, 15N/14N ratios of nitrate and ammonium in rain at Pretoria, South Africa *in* Atmospheric Environment, 21(4), 843-852 p.

Heaton, T.H.E., Spiro, B., Madeline, S., and Robertson, C., 1997, Potential canopy influences on the isotopic composition of nitrogen and sulphur in atmospheric depostion *in* Oecologia, 109, 600-607 p.

Hoering, T., 1957, The isotopic composition of the ammonia and the nitrate ion in rain *in* Geochemica et Cosmochimica Acta, 12, 97-102 p.

Johnson, R.A. and Bhattacharyya, G.K., eds., 2006, Statistics: principles and methods: John Wiley & Sons, Hoboken NJ.

Klimchouk, A., 2004, Towards defining, delimiting and classifying epikarst: its origin, processes and variants of geomorphic evolution *in* Speleogensis and Evolution of Karst Aquifers, 13 p.

Klimek, B., 2004, Effect of long-term zinc pollution on soil microbial community resistance to repeated contamination *in* Bulletin of Environmental Contamination, 88 (4), 617-622 p.

Klute, A., 1986, Methods of Soil Analysis: Part 1 – Physical and Mineralogical Methods, 2nd Ed., Madison, WI: Soil Science Society of America, Print.

Kohl, D.H., Shearer, G.B., and Commoner, B., 1971, Fertilizer nitrogen: contribution to nitrate in surface water in a corn belt watershed *in* Science, 174(4016), 1331-1334 p.

Kreitler, C.W., 1975, Determining the source of nitrate in groundwater by nitrogen isotope studies: Austin, Texas, University of Texas, Austin *in* Bureau of Economic Geology Report of Investigation #83, 57p.

Kreitler, C.W., 1979, Nitrogen-isotope ratio studies of soils and groundwater nitrate from alluvial fan aquifers in Texas *in* Journal of Hydrology, 42, 147-170 p.

Mehlich, A., 1984, Mehlich-3 soil test extractant: a modification of Mehlich-2 extractant *in* Communications in Soil Science and Plant Analysis, 15(12), 1409-1416 p.

Miller, R.B., Heeren, D.M., Fox, G.A., Halihan, T., Storm, D.E., and Mittelstet, A.R., 2014, The permeability structure of gravel-dominated alluvial floodplains *in* Journal of Hydrology, 513, 229-240 p.

Moore, H., 1977, The isotopic composition of ammonia, nitrogen dioxide and nitrate in the atmosphere *in* Atmospheric Environment, 13, 1239-1243 p.

Oklahoma State University Office of Intellectual Property, 2004, Improved method for Electrical Resistivity Imaging.

Paerl, H.W. and Fogel, M.L., 1994, Isotopic characterization of atmospheric nitrogen inputs as sources of enhanced primary production in coastal Atlantic Ocean waters *in* Marine Biology, 119, 635-645 p.

Perrin, J., Jeannin, P.-Y., and Zwahlen, F., 2003, Epikarst storage in a karst aquifer: a conceptual model based on isotopic data, Milandre test site, Switzerland *in* Journal of Hydrology, 279 (1-4), 106-124 p.

Plaza, C., Hernandez, D., and Garcia-Gil, A.P., 2004, Microbial activity in pig slurry-amended soils under semiarid conditions *in* Soil Biology and Biochemistry, 36 (10), 1577-1585 p.

Racs, G.J. and Fitzgerald, M.M., 2000, Nutrient heavy metal contents on hog manure – effect on soil quality and productivity,

Reddy, K.R., Overcash, M.R., Khaleel, R., and Westerman, P.W., 1980, Phosphorous adsorption-desorption characteristics of two soils utilized for disposal of animal wastes *in* Journal of Environmental Quality, 9(1), 86-92 p.

Schoenau, J.J., 2006, Benefits of long-term application of manure *in* Advances in Pork Production, 17, 153 p.

Sharp, J.M., Jr., 2007, A glossary of hydrogeological terms: Department of Geological Sciences, Austin, Texas, The University of Texas, 63 p.

Shearer, G.B., Kohl, D.H., and Commoner, B., 1974, The precision of determinations of the natural abundance of nitrogen-15 in soils, fertilizers, and shelf chemicals *in* Soil Science, 118(5), 308-316 p.

Shearer, G.B., Kohl, D.H., and Chien, S.-H., 1978, The nitrogen-15 abundance in a wide variety of soils *in* Soil Science Society of America Journal, 42(6), 899-902 p.

Smart, P.L., and Friederich, H., 1986, Water movement and storage in the unsaturated zone of a maturely karstified carbonate aquifer, Mendip Hills England *in* conference proceedings on: Environmental problems of Karst Terrains and their solutions, National Water Well Association, Ohio, 59-87 p.

Smith, D.R., Owens, P.R., Leytem, A.B., and Warnemuende, E.A., 2007, Nutrient losses from manure and fertilizer applications as impacted by time to first runoff event, Environmental Pollution, 147, 131-137 p.

Stepisnik, U. and Mihevc, A., 2008, Investigation of structure of various surface karst formations in limestone and dolomite bedrock with application of the electrical resistivity imaging *in* Acta Carsologica, 37(1), 133-140 p.

Suhadolc, M., Schroll, R., Gattinger, A., Schloter, M., Munch, J.C., and Lestan, D., 2004, Effects of modified Pb-, Zn-, and Cd-, availability on the microbial communities and on the degradation of isoproturon in a heavy metal contaminated soil *in* Soil Biology and Biochemistry, 36, 1943-1954 p.

Turner, J.C., Hattey, J.A., Warren, J.G., and Penn, C.J., 2010, Electrical conductivity and sodium adsorption ratio changes following annual applications of animal manure amendments *in* Communications in Soil Science and Plant Analysis, 41, 1043-1060 p.

U.S. Geological Survey, 2015, Water Science Glossary of Terms (The USGS Water Science School), accessed July 1, 2015, at URL http://water.usgs.gov/edu/dictionary.html

U.S. Geological Survey, 2014, Geologic Glossary (USGS Geology in the Parks), accessed July 1, 2015, at URL http://geomaps.wr.usgs.gov/parks/misc/glossarya.html

U.S. Salinity Laboratory Staff, 1954, Diagnosis and Improvement of Saline and Alkali Soils *in* USDA Agriculture Handbook No. 60., 84-89 p.

Williams, P.W., 1985, Subcutaneous hydrology and the development of doline and cockpit karst. Zeitschrift fur Geomorphologie, 29, 463-482 p.

Williams, P.W., 2008, The role of the epikarst in karst and cave hydrogeology *in* International Journal of Speleology, 37(1), 10p.

Wolterink, T.J., Williamson, H.J., Jones, D.C., Grimshaw, T.W., and Holland, W.F., 1979, Identifying sources of subsurface nitrate pollution with stable nitrogen isotopes: U.S. Environmental Protection Agency, EPA-600/4-79-050, 150 p.

10.0 Electronic Appendices

Appendix 1: Geodetic Data (Microsoft Excel format)

Appendix 2: ERI raw modeled data (Microsoft Excel format)

Appendix 3: ERI images (PDF format)

Appendix 4: 3D Site Models (RockWare RockWorks format)

Appendix 5: Site Photos (PDF format)

Appendix 6: Soil Analysis (Microsoft Excel format)